International Journal of
Physical and Chemical Sciences
https://www.ioro.org/ijpcs

Adsorption of Methylene Blue and Methyl Orange Dyes From Aqueuos Solution Using Activated Carbon of Jute and Sickle Senna Leaves

Hassan Salisu Nahuche [1], Magaji Ladan[2]

[1]*Research student*, [2]*Associates professor*

[1,2] *Department of Pure and Industrial Chemistry, Bayero University Kano, Nigeria.*

Abstract

Adsorption is potentially an attractive methodology for removal of hazardous dyestuff from industrial effluents. In this study, the removal efficiency of industrially important dyes methylene blue (MB) and methyl orange (MO) from aqueous solution using jute leaves (JL) and sickle senna leaves (SSL), and activated carbon of jute and sickle senna leaves A C-SSL and AC-JL as Adsorbents had been investigated. The prepared adsorbents were characterized using Fourier Transform Infrared (FTIR) spectroscopy, Scanning electron microscopy (SEM) and Energy Dispersive X-ray, (EDX). The effect of different parameters such as contact time, temperature, initial dye concentration, adsorbent dosage and pH were studied. The results obtained revel that the optimum time at 60 minutes and 50 minutes, acidic pH of 2 and 0.5g and 0.6g respectively, the experimental data were interpreted and studied using. Four isotherm models namely Langmuir, Freundlich, Temkin and Dubenin Redushkebich were tested and adsorption was found to fit well into Langmuir model and Temkin relatively better than others. The maximum loading capacity (qm) of the adsorbent AC-MOJLA is 248 and AC-MBJLB is 245 respectively. Adsorbtion kinetics parameters such as Pseudo first order, Pseudo second order, Intra particles diffusion and Simple elovich were used to described the data, the investigations showed that the kinetic data was well described by Pseudo first order and Pseudo second order kinetic model with the high correlation coefficients (R^2). Thermodynamic parameters such as change in free energy ΔG, enthalpy change ΔH, and entropy change ΔS, were calculated. The negative values of ΔG, indicate that the process is spontaneous in nature and the positive values of ΔH, shows the endothermic nature of the process. The positive values of ΔS indicated that the randomness of the solid/solution interface increased during the adsorption process. The activation energy also was calculated. The FTIR and SEM analyses of the adsorbent suggest that adsorption of the dyes was through an electrostatic interaction between the functional groups present in the dyes and those on the surface of the adsorbent. The results of the presents study substantiate that the bio- waste based materials of JL and SSL is promising adsorbents for the removal of methylene blue and methyl orange dyes.

1. INTRODUCTION

BACKGROUND OF THE STUDY

Nowadays industrial dye in the effluent has released large quantities of toxic chemicals to the water system that adversely affected the human beings as well as the living organisms. Dyes are used in various industries such as textiles, rubber, plastics, printing, leather, cosmetics, and also in production of colored products. Large amounts of these dyes are discharged into the water system, which most of the sources are coming from textile industries, it passes a serious problem to human being and living organisms in the water, it causes skin infections such as allergic, dermatitis, skin irritation, and cancer, (Bello and Semire, 2016). The

International Journal of Physical and Chemical Sciences (IJPCS)
Volume 1 | Issue 1 | 2026 | Article ID: 1039-9839-3841 | https://doi.org/10.64823/ijpcs.2601005
IORO Publications · Texas, USA · www.ioro.org

continuous increases of these dyes in the water streams by industrial technology and agricultural activities results in environmental pollution, which causes various sicknesses to human being and also causes some damages to the aquatic life.

These dyes may also be discharged into streams, rivers and lakes and the continuous movement of waters with these wastes beyond the healthy level, leading to various sicknesses to living organisms, Among the various treatment methods such as Fenton biological treatment, biodegradation, integrated chemical, biological process, electrochemical process, adsorption process, chemical coagulation flocculation degradation process etc. have been explored to remediate these dyes in the wastewater. Among the various techniques available for its remediation adsorption technique has been proved to be most effective. Adsorption is preferred over other processes due to possible regeneration, sludge free operation and recovery of the sorbet. The most commonly used adsorbent in the adsorption process is activated carbon. Activated carbon has the advantage of exhibiting a high adsorption capacity for color pollutants due to their high surface area and porous structure (Audu *et al*., 2014).

Today natural agricultural biodegradable materials are used widely for the detection and removal of chemical substances such as dyes (e.g methylene blue, methyl orange, congo red and alizarin red s) metals (e.g lead, cadmium, copper and zinc (Amin., 2008*)* organic and inorganic contaminants of concern from waste water systems which include naphthenic acids (NA), ammonia, chromium (VI), sulfates, aromatic hydrocarbons, and trace metals. (Puthoor,. 2017).

2. LITRATURE REIEW

ADSORPTION OF DYES USING DIFFERENT ADSORBENTS

Ladan *et al*., (2013). Investigate the thermodynamic properties of chromium adsorption by sediments of river watari, Kano State; the adsorption parameter such as influence of initial pH, solution temperature, adsorbent and adsorbate concentrations on the adsorption efficiency was investigated using batch equilibrium, the results obtained for the adsorption potential was recorded at initial pH of 2 and a temperature of 25°C. The experimental data obtained for the adsorption were described by the following isotherm models which includes; Linear, Langmuir, Freundlich and Temkin to establish the mechanism of chromium adsorption onto the sediment. Amongst the four models tested, Langmuir gave the best fit with regression values ranging from 0.6494 to 0.7459 for 25°C, 30°C, 40°C and 50°C respectively which indicate the homogeneous surface for the sediment. The isosteric heat (ΔHr) of adsorption and enthalpy change (ΔH) did not change with temperature also indicating a homogeneous sediment surface. Based on the values of entropies, activation energies and Gibb's free energies obtained, the adsorption was found to be spontaneous at all temperatures.

In another study, Yunus *et al*., (2020). Carried out a series of investigation on the adsorption of malachite green on the activated carbon of desert date seeds shells, the following parameters were determined, pH, contact time, dosage, initial concentration and temperature, Experimental data were analyzed using five kinetic models: pseudo-first-order, pseudo-second-order, Elovich, intraparticle diffusion and Boyd models and it was found that the pseudo-second-order model fitted the adsorption data most with the highest correlation (R2 = 0.9999). The overall adsorption process appears to be jointly controlled by intra particle diffusion and film diffusion mechanisms. From the Studies, thermodynamic behavior revealed negative values for ΔG (-11.45 to -13.42 kJ mol^{-1}), and a positive value for ΔH (8.39 kJ mol-1) and ΔS (0.065 kJ mol-1 K-1). These indicated the feasibility, endothermicity and spontaneity of the removal process. The results demonstrated that the adsorbent could be exploited in the removal of MG from aqueous solution.

Haddad *et al*., (2002). Studied the adsorption behavior of MB onto mesoporous carbon material of Rice husk with a Brunauer-Emmett- Teller (BET) surface area of 951m^2/g and a pore volume of 0.97cm3/g. The adsorption capacity was 335 mg/g at a pH of 3. This study also reported an increase in adsorption capacity with a decrease in pH due to increase in positive charges on the surface favoring the adsorption of anionic.

Ayuba *et al*., (2021). Performed a series of experiment on adsorption of Congo red dye from aqueous solution onto activated cowpea, (*Vigna unguiculata*) husk. The results showed that maximum adsorption capacity was obtained at the optimum levels of contact time (24.3157mg/g at 60 minutes), adsorbent dose (24.532mg/g at 0.1g), initial dye concentration (407.2787mg/g at 500mg/L) and pH (24.26mg/g at 1.5). Adsorption equilibrium data were represented by isotherm, kinetics and thermodynamics models. Three isotherm models namely Langmuir, Freundlich and Temkin were tested and adsorption was found to fit well into Langmuir model relatively better than others. The maximum loading capacity (qm) of the adsorbent for Congo red obtained from the Langmuir isotherm model is 263.16 mg/g. The kinetic data was well described by the pseudo second order kinetic model with the correlation coefficients (R2) value of 0.994. The adsorption process was found to be thermodynamically endothermic and spontaneous. The negative value of ΔS (-0.00053J/mol.k), indicate that, the randomness decreases at the adsorbent/adsorbate interface during the adsorption process. FTIR and SEM analyses of the adsorbent suggest that adsorption of the dye was through an electrostatic interaction between the functional groups present in the dye and those on the surface of the adsorbent.

Senthil and Kumar (2005). Evaluated the removal of methylene blue on the activated carbon of rice husk; the adsorption parameters such as time contact, concentration, pH solution, and sorbent dosage were determined and play an important role in removing MB in water media. The results showed that the MB adsorption efficiency reached over 80 % at a concentration of 50 mg/L, pH 8 within 180 minutes. The kinetic analysis via Pseudo-first-order, Pseudo-second-order, Bangham, and Temkin model showed that MB adsorption followed pseudo-second-order (R^2 = 0.99934). The fitness of equilibrium data to popular isotherm equations such as the Langmuir, Freundlich, Elovich, Temkin and Dubinin-Radushkevich were carried out. Among all tested isotherm models, Langmuir model is the best fitted to equilibrium data (R^2 = 0.99924). The results of this study show that activated carbon made from rice husk has the potential to be used to remove the dye in waste water treatment.

3. MATERIALS AND METHODS

3.1. METHODS

3.1.1. Sample Collection

Jute leaves and sickle senna leaves were collected from Nahuche town, zamfara state Nigeria. the plants samples was identified in habarium laboratory, department of plants science, Bayero University kano with Habarium accession number BUKHAN 0356 for jute leaves, BUKHAN 0357 sickle senna plants with the family names *leguminosae caesalpinioiddeae*, *Corrchorus spp for jute plants*.

3.1.2. ADSORBENT PREPARATION

Jute leaves and sickle senna leaves was obtained from the farm and washed thoroughly and dried in shade for seven days and then dried in an oven for 24 hrs at 70 ℃. The samples were grinded into powder using motor and pistil.

3.1.3. PREPARATION OF ACTIVATED CARBON

The dried sickle senna and jute leaves were carbonized in the Department of Pure and industrial Chemistry Laboratory of Bayero University Kano, Kano State Nigeria.

100 g of the dried sample was placed in a muffle furnace (Carbolite Sheffield, England, LMF4) and heated at a temperature of 350^{0}C for 2 hours. During the process, the steam was removed from the oven through the exhaust pipes. Under such oxygen-deficient conditions, the biomaterial was thermally decomposed to porous carbonaceous materials and hydrocarbon compounds. After cooling the activated samples to room temperature of 25^{0}C, then wash with distilled water to constant pH of 7. The wash activated sample was dried in an oven at 105^{o}C to constant weight. The final product was kept in an air tight polyethene bags (Ojedokun and Bello., 2019). The carbonized sample was sieve through a 100-mm mesh Tyler sieves and labeled it as sickle senna and jute leaves raw samples (R).

3.1.4. PREPARATION OF STOCK SOLUTION

1g of methylene blue (373g) and 1g of methyl orange (327.33g) were taken in each 1000ppm volumetric flask and dissolved in distilled water, making it to the mark. These were 1000ppm stock solution of dyes. The standard solution of dyes, were prepared by serial dilution of the stock solution.

3.1.5. ACTIVATION OF THE CARBONIZED SAMPLES

Both acid and base activation was carried out in this study. A carefully weighed 15g of carbonized carbon and put it in a beaker containing 150 ml of 0.1 mol/ dm^3 Sulfuric acid (H_2SO_4; for acid activation) and 150 ml of 0.1 mol/dm^3 sodium hydroxide (NaOH; for base activation) respectively. The content of the beaker was carefully homogenized and allowed to stand for 24 h. The already activated sickle senna and jute leaves was diluted with 200 ml of distilled water to rinse off the activating agents (H_2SO_4 and NaOH) that was used for impregnation. The process of washing was repeated until the pH falls between 6.5 and 7.0. It was oven dried at 105^{0}C for 4 hrs to constant weight, then sieved with a 106 mm mesh to obtain fine powdered sickle senna and jute activated carbon for both acid (SSLA&JLA) and base (SSLB&JLB) respectively. Then kept it in airtight container and used for further user.

3.2. CHARACTERIZATION

3.2.1. FTIR SPECTROSCOPY

The surface functional groups of the samples SSL, JL and AC-SSLA, SSLB, JLA and JLB were identify using Fourier transform infrared spectroscopy (FTIR) to study the functional group of both raw and activated sickle senna and jute leaves, (FTIR-2000, Perkin Elmer model). FTIR spectra was recorded between 4000 and 400 cm^{-1}. The discs will be prepared first by mixing 1 mg of dried sample with 500 mg of KBr (Merck, for spectroscopy) in an agate mortar and then pressing the resulting mixture at 10 tones cm^{-2} for 15 min under vacuum. The FTIR spectra give information about the characteristic functional groups on the surface of raw and activated sickle senna and jute leaves.

3.2.2. SCANNING ELECTRON MICROSCOPY (SEM)

SEM is a type of microscope which uses a beam of highly energetic electrons to scan sample and produce its image. It consists of electron gun which acts as a source for electrons. The electron

beam is focused by a pair of condenser lenses made of magnets which are capable of bending the path of electrons. Sample to be analyses is placed in the sample chamber. The electron beam strikes the sample gets decelerated and produces a variety of diffracted backscattered electrons, protons, visible light and heat. The secondary electrons are picked up by the electrons & produces images of the object's surface on the monitor. The entire operation takes place in the vacuum chamber. The activated carbon can be analyzed in a SEM to visualize the porous structure. The magnification is analyzed and adjusted so as to get a clear picture.

3.3. ADSORPTION EXPERIMENT

The batch adsorption experiment was conducted to evaluate the effects of various factors including adsorbent dosage (0.1- 1g), pH (2- 10), contact time (10-50 minutes), initial concentration (10-50mg/L) and temperature (25 °C-60 °C) on the adsorption of MB and MO using SSL, JL and AC-SSLA, SSLB, JLA and JLB. All the experiments were perfumed at the laboratory temperature (30 °C) with the exception of effect of temperature were shacked at 200 rpm in a 100ml sample bottles. After agitation time, the suspension was filtered through a filter paper and the absorbance of the clear samples was analyzed to determine the remaining MB and MO. The amount of MB and MO absorbed on SSL, JL and AC-SSLA, SSLB, JLA and JLB respectively and the adsorption percentage removal (%) were computed using the following equations:

$$\% \text{ Removal} = C_o - C_e / C_O \times 100\% \quad (7)$$

$$\text{And} \quad Q_e = C_o - C_e / M \times V \quad (8)$$

Where C_o and C_e are the concentrations (mg/l) of the dyes initially and at equilibrium time, M is the mass of the adsorbent dosage and V is the volume.

3.3.1. FREUNDLICH ISOTHERM:

It is an adsorption isotherm which relates concentration of solute on the surface of the adsorbent to the concentration of the solute in the liquid with which it is in contact. This model assumes that adsorption takes place on heterogeneous surface.

The linear form of the equation can be written as:

$$\text{Log } Qe = \log kf + (1/n) \log Ce \quad (2)$$

Where, kf and n (dimensionless constants) are the Freundlich adsorption isotherm constants, which indicate the capacity and intensity of the adsorption, respectively (Bello *et al.*, 2012).

3.3.2. LANGMUIR MODEL

It relates the adsorption of molecules on a solid surface to gas pressure or concentration of a medium above the solid surface at a fixed temperature. It's based upon the fact that adsorption process occurs in monolayer.

The linear form of Langmuir expression: $1/Qe = 1/Qo + 1/ bQoCe \quad (3)$

Where Ce is the equilibrium concentration of dye solution (mg/L), Qe is the equilibrium capacity of dye on the adsorbent (mg/g), Qo is the monolayer adsorption capacity of the adsorbent (mg /g), and b is the Langmuir adsorption constant (L/mg) and is related to the free energy of adsorption. (Bulut *et al.*, 2020).

3.3.3. DUBININ-RADUSHKEVICH

isotherm model is another empirical model which initially formulated for the adsorption process following a pore filling mechanism. It is generally applied to express the adsorption process occurred onto both homogeneous and heterogeneous surfaces. The non-linear expression of Dubinin-Radushkevich isotherm model can be illustrated as Equations,

$$Qe = Qs \exp(-KDR\ E2) \quad 4$$

$$E2 = RT \ln(1 + 1/Ce) \quad 5$$

where Qs (mg P/g) is a constant in the Dubinin-Radushkevich isotherm model which are related to adsorption capacity; Qe is equilibrium Concentration, KDR (mol-1/kJ-1) is a constant in related to the mean free energy of adsorption; R (J/mol K) is the gas constant; and T (K) is the absolute temperature. (Ahmad *et al.*, 2011).

3.3.4. TEMKIN MODEL

Like the Freundlich isotherm, it assumes that the adsorption heat of all molecules decreases linearly when the layer is covered and that the adsorption has a maximum energy distribution of a uniform bond. The linear form of Temkin equation can be given as

$$Q_e = B \ln KT + B \ln Ce \quad 6$$

Where bT and KT are the Temkin constants, R the universal gas constant (8.314J/molK), and T is the absolute solution temperature in Kelvin.

KT is the equilibrium binding constant (L/mol) corresponding to the maximum binding energy, and bT is the variation of adsorption energy (J/mol), and also its related to the heat of adsorption process, where the positive or negative value of bT shows that the adsorption process is exothermic or endothermic process, respectively. B is related to the heat of adsorption and equals RT/bT. A linear plot of qe versus ln Ce gives the value of constants B and KT from the slope and intercept, respectively. (Gimba *et al.*, 2007).

3.3.5. EFFECT OF INITIAL CONCENTRATION

Equilibrium studies were carried out by using 0.6g of sickle senna and jute leaves activated carbon with 50 ml of dyes solutions of different concentration (10, 20, 30, 40 and 50 mg/L) in 200 ml sample bottles at constant (pH of 2), the samples were shaken at a constant oscillation of 115 rpm and 35 ℃. The experiment was repeated for 1gm of prepared sample.

Samples were collected after 50 minutes. The % absorbance at 664 and 464 nm was found out using a UV-spectrophotometer (Audu *et al.*, 2014).

3.3.6. EFFECT OF ADSORBENT DOSAGE

Keeping the pH of the dyes solution constant (pH of 2), the following results obtained earlier: 0.2, 0.4, 0.6, 0.8 & 1gm of SSL, JL and AC-SSLA, JLA, SSLB were added to 100 ml of 20 mg/L of dyes solution and then shakes at constant oscillation of 115 rpm for 40 minutes at 35℃. Then the samples were allowed to settle down after which it's filtered, the % absorbance at 664 and 464 nm was found out using a UV-spectrophotometer (Ayuba et al., 2020)

3.3.7. EFFECT OF CONTACT TIME

0.6 gm. of SSL, JL and AC-SSLA, SSLB, JLA and JLB were added to 100 ml of 20 mg/L ml of the dye's solution in a flask at constant (pH of 2), the samples were agitated for the time of (20, 30, 40, 50 & 60 min), in sample bottle at a constant oscillation of 115 rpm, at a temperature of 35℃. The % absorbance was found using UV spectrophotometer at 664 and 464 nm (Pathoor.,2017).

3.3.8. EFFECT OF PH

The effect of pH was studied by varying the pH of 2, 4, 7, and 10.0 Samples for MB dyes and it was also studied by varying the pH to 2, 4, 6, 8 and 10. of mo, 0.1g of adsorbent was added to each of 100ml dye solution containing 10mg/L of dye at the room temperature and adsorption was studied at an adsorption time of one hour with constant shaking. The pH was adjusted by adding sulphuric acid and sodium hydroxide solution.

The % absorbance at 664 and 464 nm was found out using a UV-spectrophotometer (Gimba and Musa., 2007)

3.3.9. EFFECT OF TEMPERATURE

The effect of temperature was carried out by varying the temperature (30℃, 40℃ 45℃, 50℃, 60℃) at constant (pH of 2) initial concentration of 30mg/L and 0.6g of the adsorbent. The after equilibrium, the concentration was analyzed (Bello and Ahmad., 2011a)

3.4. KINETICS STUDIES

For the determination of mechanisms of the adsorption such as mass transfer and chemical reactions, Pseudo first order, Pseudo second order, Simple elovich and Intra particle diffusion were used to test the experimental data of methylene blue and methyl orange adsorption on SSL, JL and AC-SSLA, SSLB, JLA, and JLB.

3.4.1. The pseudo first order equation is represented as:

$$\text{Log qe - qt = log qe – k1t /2.303} \qquad 15$$

Where qe (mg/g) is the amount of dyes adsorbed at equilibrium, qt (mg/g) is the amount of dye adsorbed at a time t and k is the rate constant of pseudo first order. A straight line is obtained by plotting log (qe-qt) versus t indicate the application of pseudo first order kinetics model whereas in true first order log q should be equals to the intercept (Susmita *et al*. 2014).

3.4.2. The pseudo second order equation based on adsorption equilibrium capacity may be represented as follows

$$\frac{t}{K_2}=\frac{1}{K_{2Qe}}+\frac{1}{Q_e}t \qquad 16$$

By plotting $\frac{t}{qt}$ versus t give a linear relationship from which qe and k2 can be determined from the slope and intercept of the plot.

3.4.3. The Elovich equation is given as follows

$$\frac{dqt}{dt}=ae\beta\text{qt} \qquad 17$$

The integration of the rate equation with the same boundary conditions as the pseudo first- and second-order equations becomes the Elovich equation.

$$qt = \frac{1}{\beta} \in (\alpha\beta) + \frac{1}{\beta} \int ¿ \quad 18$$

Where α is the initial sorption rate (mg.g-1 min-1), and the parameter β is related to the extent of surface coverage and activation energy for chemisorptions (g/mg).

3.4.4. The intra-particle diffusion model is expressed as (Weber and Morris, 1963; Srivastava *et al.*, 1989) $R = kid(t)a$ A linearises form of the equation is followed by

$logR = logkid + alog(t)$: If (MB) adsorption fits the intraparticle model, a plot of log R vs. log t should yield a linear relationship with a slope of and an intercept of log kid.

The fractional approach to equilibrium changes according to a function of

(Dt/r2)1/2, $(Dt/r2)$ 19

Where;

R is the particle radius and D the diffusivity of solute within the particle.

The rate parameter (kint) for intra particle diffusion can be defined as:

Qt = kint t1/2 + I 20

Where kint is the intra particle diffusion rate constant ($mg.g^{-1}$ $min^{1/2}$) and I is the boundary layer ($mg.g^{-1}$)

3.5. THERMODYNAMICS STUDIES

During the present studied, thermodynamic parameters, i.e. free energy change, (ΔG), enthalpy change (ΔH) and entropy change (ΔS), were calculated using empirical equations

$\Delta G = - RT\, InK_c$ 9

$\Delta G = \Delta H - T\Delta S°$ 10

$$Log K_C = \frac{\Delta G}{RT} \quad 11$$

$\Delta S ¿ \Delta H^{-¿ \Delta G/T ¿}$

$Ink_1/k_2 = Ea / R\ (1/T_1 - 1/T_2)$ 12

$\Delta H = Ea - nRT$ 13

The thermodynamic parameters that must be considered to determine the process are changes in Gibbs free energy (ΔG°), standard enthalpy (ΔH°), and standard entropy (ΔS°) due to transfer of unit mole of solute from solution onto the solid–liquid interface. The Gibbs free energy change of adsorption is defined using Vant Hoff equation.

$\Delta G° = RT \ln K_l$

Where Kl is Langmuir equilibrium constant (g/lit), (R) is the universal gas constant (8.314 $J.mol^{-1}.K^{-1}$) and (T) is the absolute temperature (K).

4. RESULT

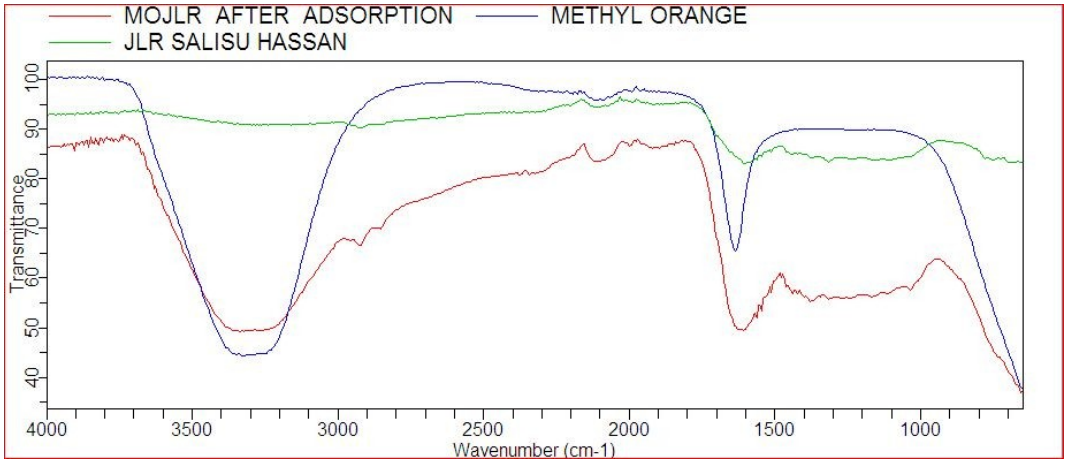

Figure 4.1: FTIR Spectrum of (a) MO, (b) JLR before and (c) JLR after Adsorption.

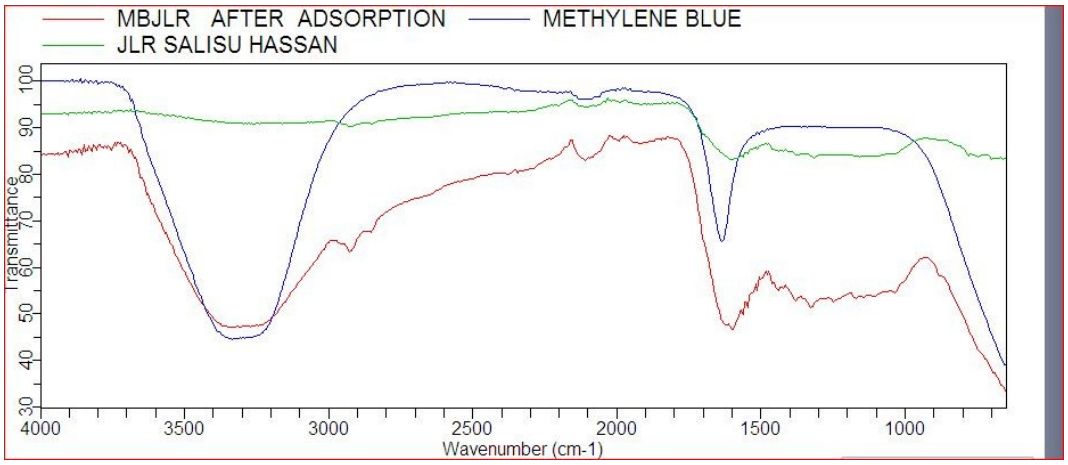

Figure 4.2: FTIR Spectrum of (a) MB, (b) JLR before and (c) JLR after Adsorption.

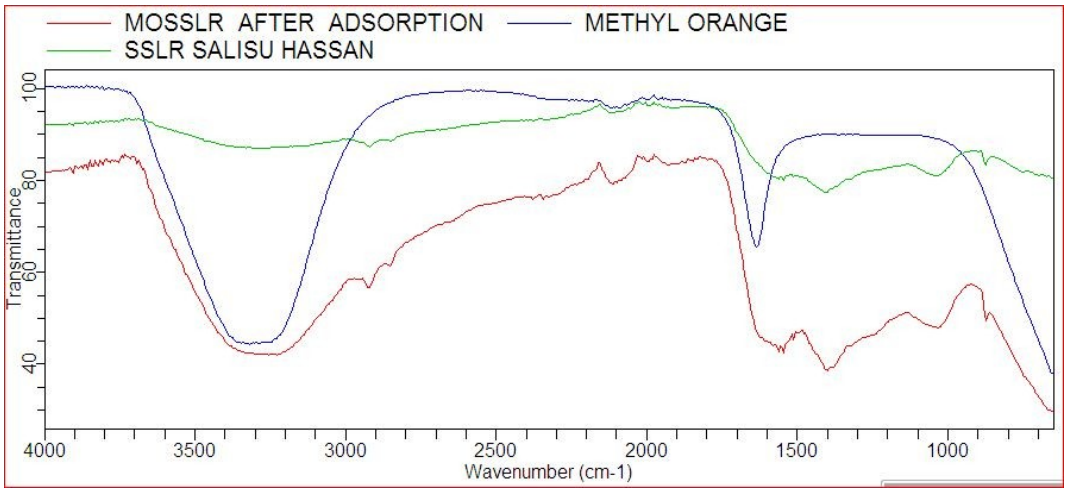

Figure 4.3: FTIR Spectrum of (a) MO, (b) SSLR before and (c) SLR after Adsorption.

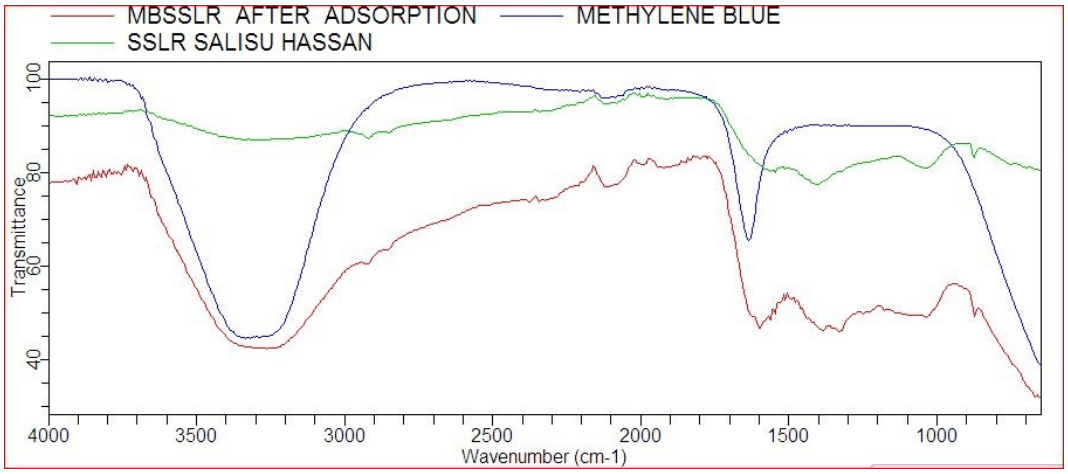

Figure 4.4: FTIR Spectrum of (a) MB, (b) SSLR before and (c) SSLR after Adsorption.

The various functional groups that might participate in the adsorption of MB and MO onto AC-MBSSLR, MOSSLR and MBJLR, MOJLR were elucidated using FTIR analysis. The figure above reveals changes in terms of less complexity as fewer functional groups were observed some peaks seen in the AC-MBSSLR and MOSSLR were not observed in the AC-MBJLR and AC-MOJLR probably due to elimination of some functional groups during the pyrolysis. After the thermal treatment, appreciable changes were observed in terms of decreased in the intensity of some peaks while others have slightly shifted their position.

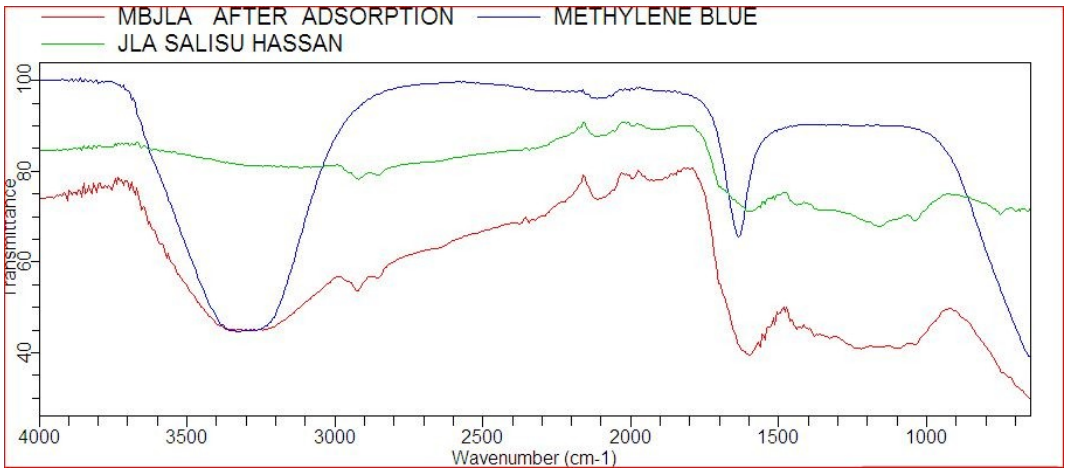

Figure 4.5: FTIR Spectrum of (a) MB, (b) JLA before and (c) JLA after Adsorption.

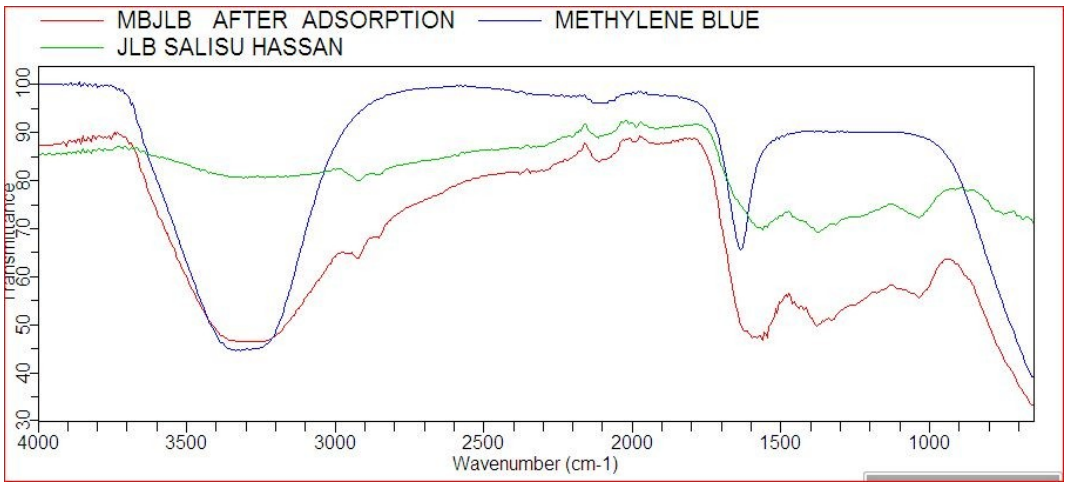

Figure 4.6: FTIR Spectrum of (a) MB, (b) JLB before and (c) JLB after Adsorption.

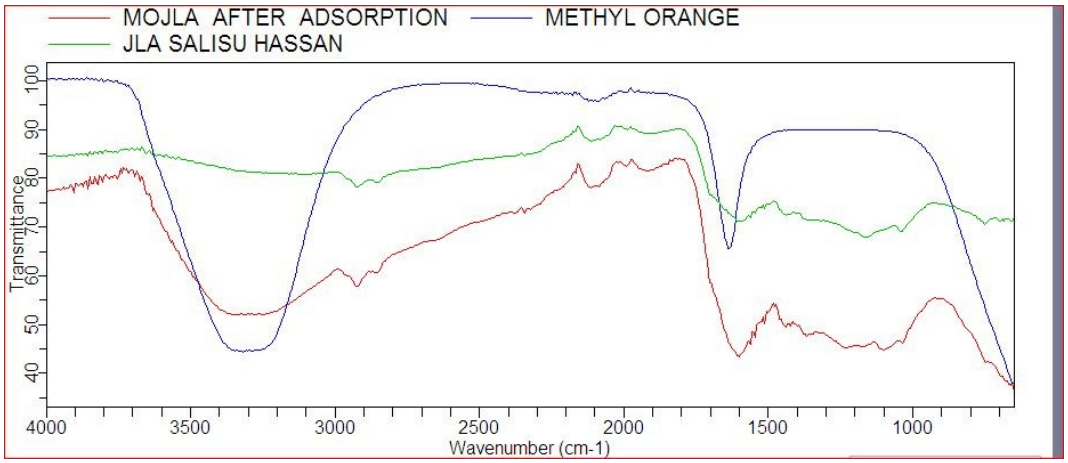

Figure 4.7: FTIR Spectrum of (a) MO, (b) JLA before and (c) JLA after Adsorption.

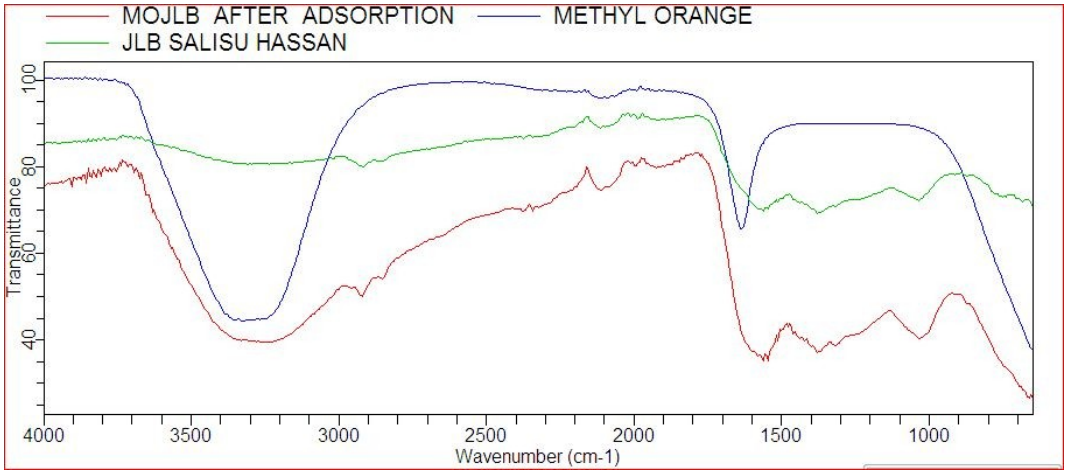

Figure 4.8: FTIR Spectrum of (a) MO, (b) JLB before and (c) JLB after Adsorption.

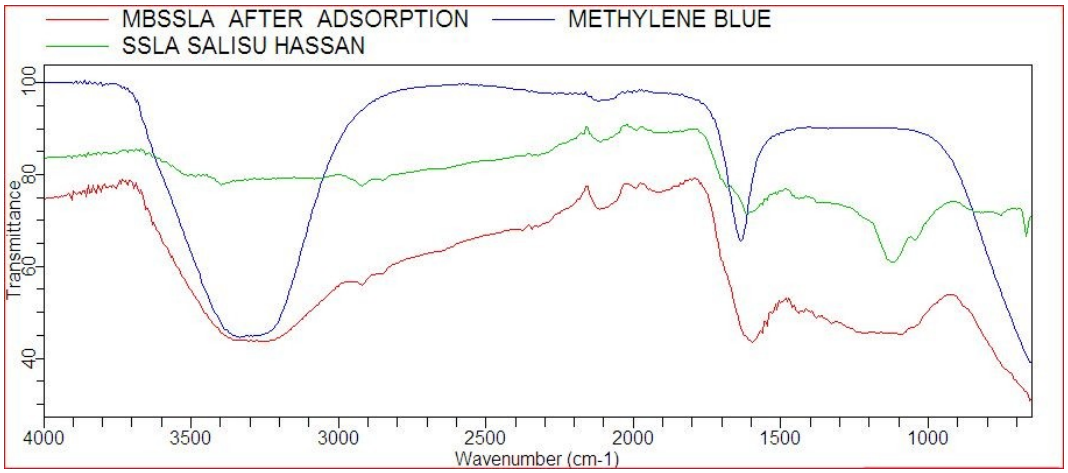

Figure 4.9: FTIR Spectrum of (a) MB, (b) SSLA before and (c) SSLA after Adsorption.

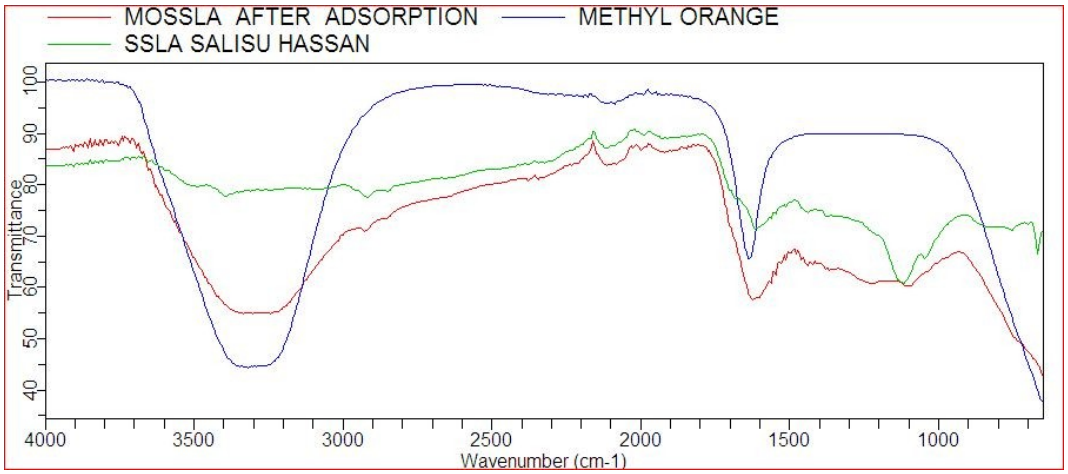

Figure 4.10: FTIR Spectrum of (a) MO, (b) SSLA before and (c) SSLA after Adsorption.

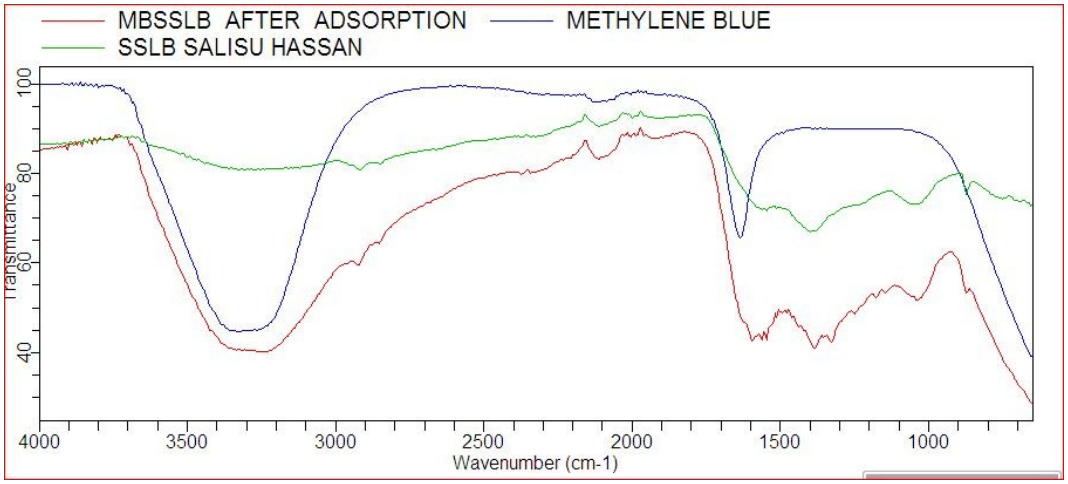

Figure 4.11: FTIR Spectrum of (a) MB, (b) SSLB before and (c) SSLB after Adsorption.

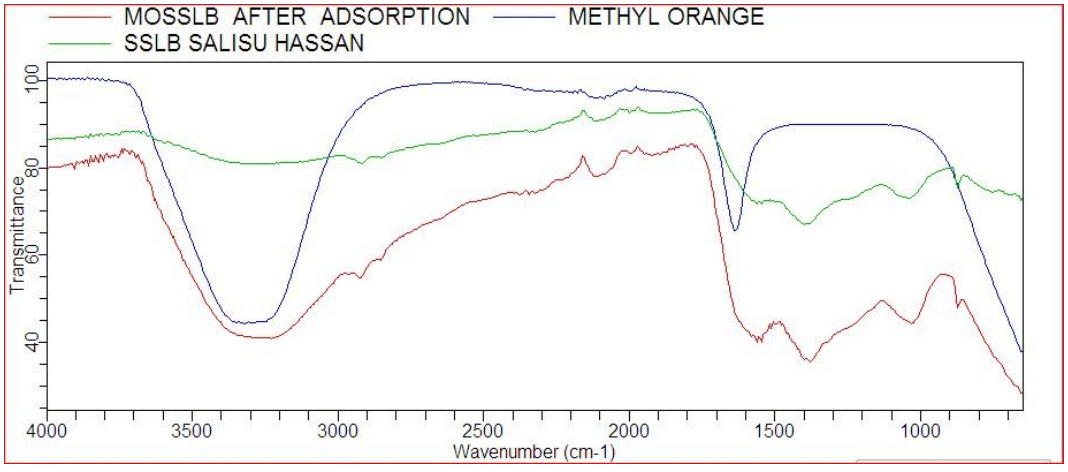

Figure 4.12: FTIR Spectrum of (a) MO, (b) SSLB before and (c) SSLB after Adsorption.

Figure 4.4 to 4.8: FTIR spectrum of MO and MB dyes on AC MB JLA, JLB, MOJLA, JLB, and MBSSLA, MOSSLA, MBSSLB and MOSSLB respectively before and after adsorption, the various functional groups that might participate in the adsorption of MB and MO onto SSL and JL were elucidated using FTIR analysis. The figure above shows the presence of so many functional groups before and after activation with acid appreciable changes were observed in terms of increased in the intensity of some peaks while others have slightly shifted their position, the various functional groups also that might participate in the adsorption of MB and MO onto

AC-MBSSLA, MBSSLB, MOSSLA and MOSSLBJL were elucidated using FTIR analysis. The figure above reveals changes in terms of less complexity as fewer functional groups were observed some peaks seen in the AC-MBSSLA, MOSSLA were not observed in the AC-MBSSLB, MOSSLB and also peaks seen in AC-MBJLA, MOJLA were not observed in AC-MBJLB, MOJLB respectively probably due to elimination of some functional groups during the pyrolysis. After thermal treatment some changes were observed in terms of decreased in the intensity of some peaks while others have slightly shifted their position

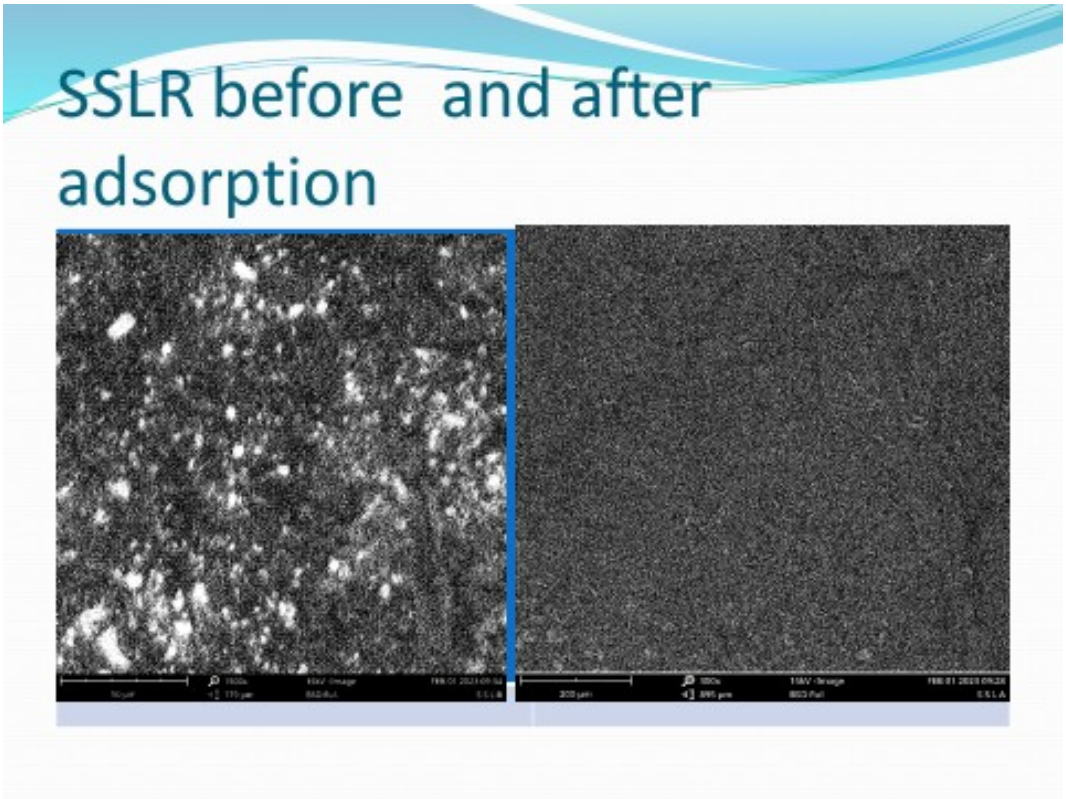

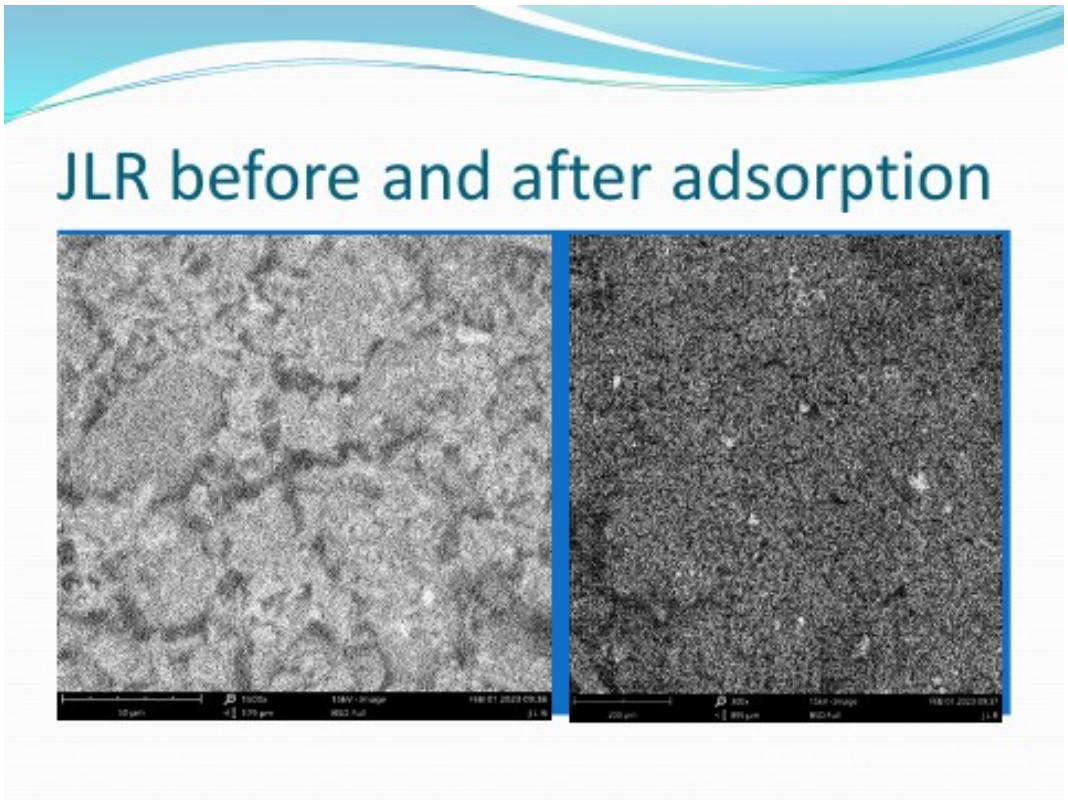

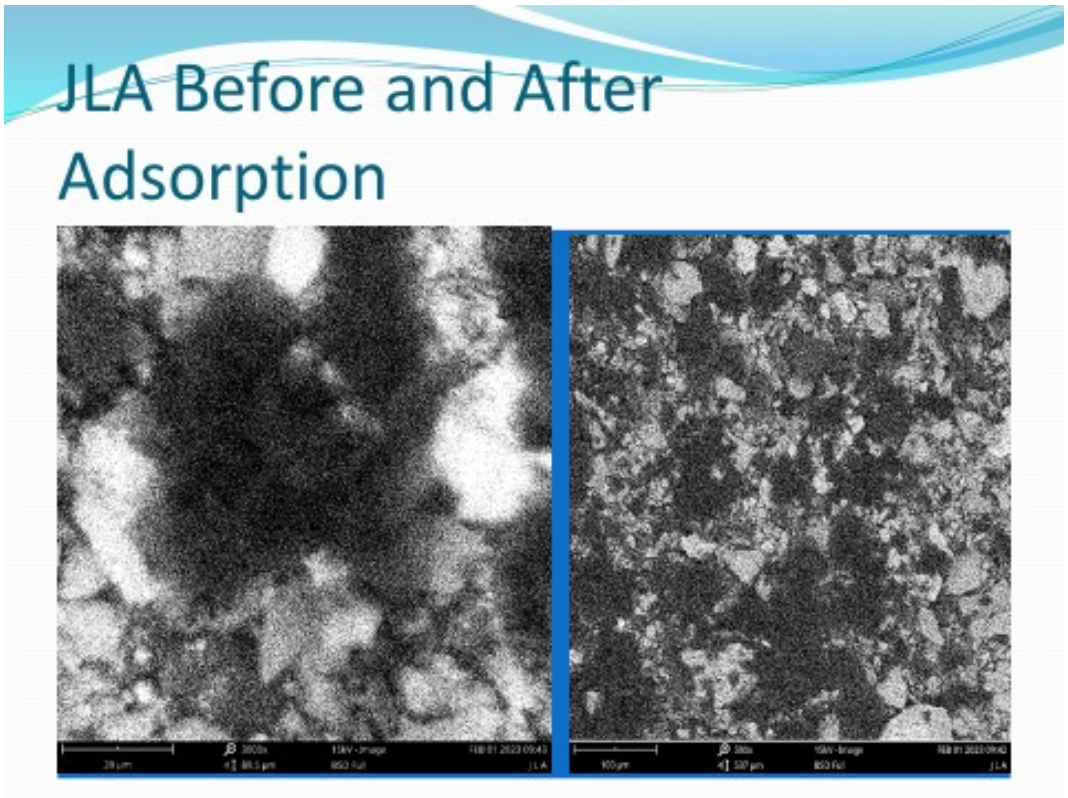

Figure 4.15: SEM micrograph of JLA, before and after adsorption.

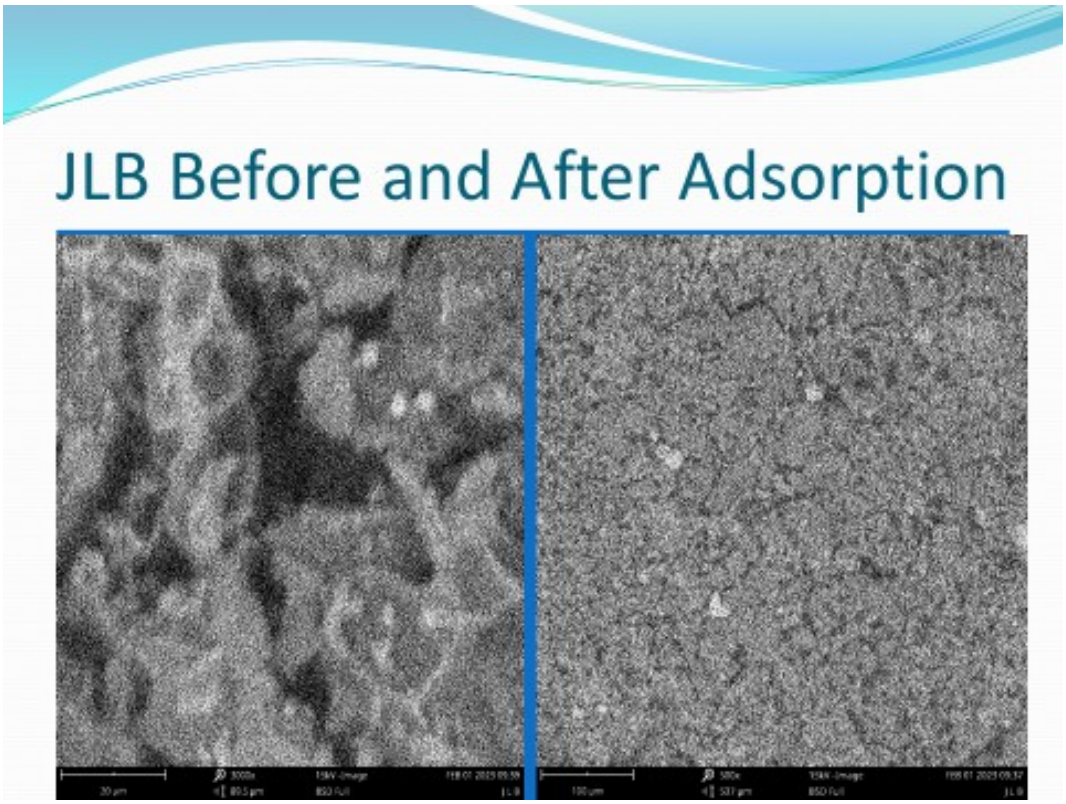

Figure 4.16: SEM micrograph of JLB, before and after adsorption.

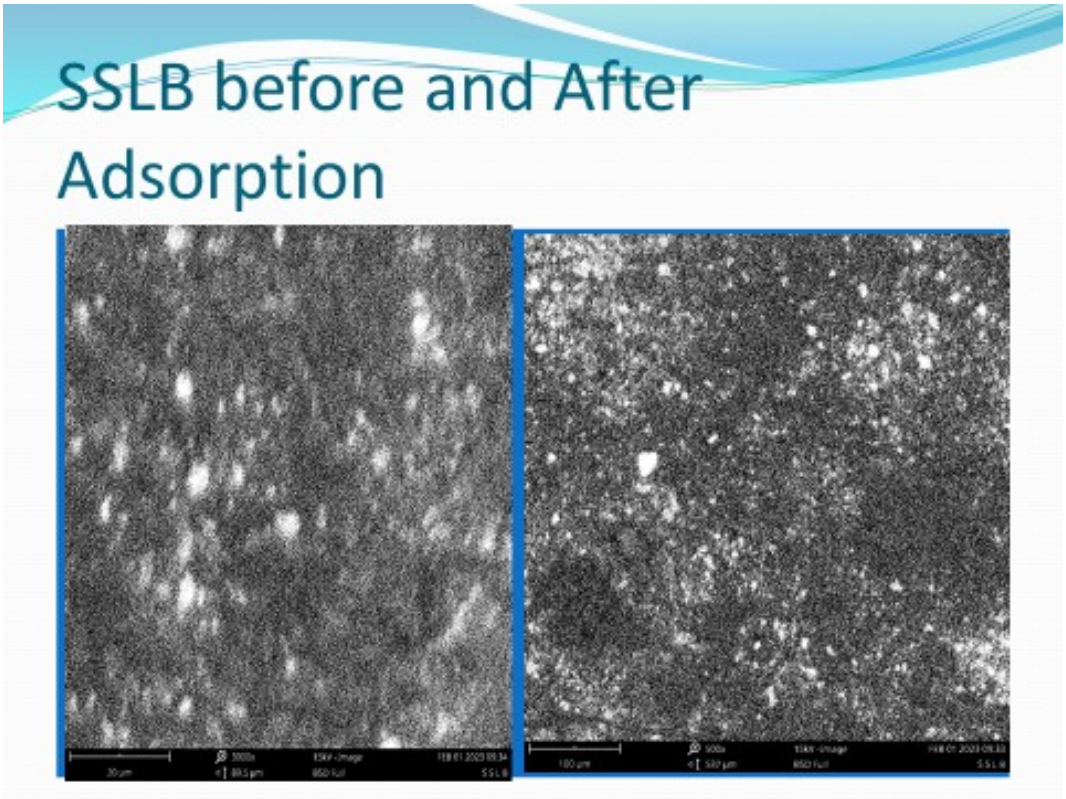

SEM Microscopic images of precursor SSL, JL and AC-SSLA, SSLB, JLA and JLB before and after Adsorption were shown in (figures 4.8-4.24) respectively.

The SSL and JL adsorbent shows a lesser elongated, rough and irregular surface with low degree of porosity (figure 4.12 and 4.16) while the AC-SSLA, SSLB, JLA and JLB represent the highly porous structure with small number microspores. After MO and MB dyes adsorption (figure 4.6-4.57 and 4.8-4.9), the pores of SSL, JL and AC-SSLA, SSLB, JLA and JLB are filled due to the adsorption of MO and MB dyes which may confirm the adsorption phenomenon between the MO and MB dyes and SSL, JL and AC-SSLA, SSLB, JLA and JLB respectively.

Table 4.2: Thermodynamics parameters for methylene blue dye, Enthalphy (ΔH^o), Entrphy (ΔS^o) and Free energy change (ΔG^o).

Sample	Ea(J/mol)	LnKl	T(K)	ΔH^o(kJ/mol)	ΔS^o(J/mol/K)	ΔG^o(kJ/mol)
SSLA	**$3.85x10^4$**	5.11	299	42.70	0.110	-12.78
	$3.33x10^4$	5.14	303	42.68	0.190	-12.94
	$2.86x10^4$	5.63	308	55.45	0.180	-17.08
	$2.50x10^4$	6.64	313	55.54	0.180	-17.38
	$2.22x10^4$	6.86	318	49.80	0.180	-18.08
SSLB	**$3.85x10^4$**	5.35	299	44.48	0.150	-13.29
	$3.33x10^4$	5.39	303	44.89	0.070	-13.58
	$2.86x10^4$	5.48	308	45.8	0.080	-14.08
	$2.57x10^4$	5.72	313	47.56	0.150	-14.88
	$2.22x10^4$	5.99	318	47.71	0.160	-15.84
JLA	**$3.85x10^4$**	5.32	299	44.23	0.150	-13.22
	$3.33x10^4$	5.44	303	45.23	0.150	-13.70
	$2.86x10^4$	5.52	308	45.89	0.850	-14.14
	$2.5x10^4$	5.97	313	49.72	0.160	-15.56
	$2.22x10^4$	7.85	318	65.18	0.210	-20.73

JLB	**$3.85x10^4$**	5.48	299	45.56	0.150	-13.62
	$3.33x10^4$	5.76	303	47.89	0.160	-14.51
	$2.86x10^4$	6.27	308	52.13	0.160	-16.06
	$2.5x10^4$	6.99	313	58.19	0.190	-18.22
	$2.22x10^4$	8.49	318	70.59	0.220	-22.45

Table 4.3: Thermodynamics parameters for methyl orange dye, Enthalphy (ΔH°), Entrophy (ΔS^O) and Free energy change (ΔG^O)

Sample	Ea(J/mol)	Lnkl	T(K)	ΔH°(kJ/mol)	ΔS°(J/mol/K)	ΔG°(kJ/mol)
SSLA	**$3.85x10^4$**	4.51	299	37.25	0.120	-11.14
	$3.33x10^4$	5.55	303	45.8	0.160	-13.88
	$2.86x10^4$	5.75	308	47.47	0.150	-14.67
	$2.5x10^4$	6.06	313	50.03	0.185	-15.67
	$2.22x10^4$	6.23	318	51.43	0.160	-16.34
SSLB	**$3.85x10^4$**	4.78	299	39.47	0.150	-11.80
	$3.33x10^4$	5.15	303	42.52	0.140	-12.88
	$2.86x10^4$	5.65	308	46.67	0.160	-14.42
	$2.5x10^4$	6.01	313	49.63	0.160	-15.54
	$2.22x10^4$	6.96	318	57.53	0.180	-18.29
JLA	**$3.85x10^4$**	4.63	299	38.13	0.130	-11.40
	$3.33x10^4$	4.88	303	40.24	0.130	-12.19
	$2.86x10^4$	4.98	308	41.15	0.140	-12.72
	$2.5x10^4$	5.63	313	46.53	0.150	-14.56
	$2.22x10^4$	6.49	318	53.63	0.160	-17.05
JLB	**$3.85x10^4$**	4.76	299	39.33	0.130	-11.76
	$3.33x10^4$	5.07	303	41.90	0.140	-12.70
	$2.86x10^4$	5.53	308	45.64	0.150	-14.10
	$2.5x10^4$	5.84	313	48.22	0.140	-15.09
	$2.22x10^4$	6.55	318	54.12	0.170	-17.21

Table 4.4: Thermodynamics parameters for MB&MO dyes for the raw samples of SSLR& JLR

Sample	Ea(J/mol)	Lnkl	T(K)	ΔH°(kJ/mol)	ΔS°(J/mol/K)	ΔG°(kJ/mol)
MO JLR	$3.33x10^4$	5.21	299	43.26	0.210	-12.95
	$3.63x10^4$	5.27	303	43.81	0.150	-13.28
	$3.28x10^4$	5.46	308	45.41	0.130	-13.98
	$3.20x10^4$	5.67	313	47.31	0.150	-14.81
	$3.18x10^4$	5.77	318	48.05	0.180	-15.28
MB JLR	$3.3x10^4$	5.01	299	41.65	0.140	-12.45
	$3.3x10^4$	5.35	303	44.48	0.150	-13.48
	$3.2x10^4$	5.64	308	46.89	0.150	-14.44
	$3.2x10^4$	5.83	313	48.47	0.160	-15.17
	$3.10x10^4$	5.92	318	49.22	0.150	-15.65
MO SSLR	$3.3x10^4$	5.01	299	41.74	0.120	-12.48
	$3.3x10^4$	5.15	303	42.82	0.140	-12.97
	$3.2x10^4$	5.39	308	44.81	0.150	-13.80

$3.2x10^4$	5.69	313	47.31	0.150	-14.80
$3.1x10^4$	5.90	318	49.05	0.160	-15.59
MB SSLR $3.3x10^4$	5.10	299	42.73	0.150	-12.78
$3.3x10^4$	5.38	303	44.73	0.150	-13.55
$3.2x10^4$	5.64	308	46.89	0.150	-14.44
$3.2x10^4$	5.69	313	47.31	0.150	-14.81
$3.1x10^4$	5.79	318	48.14	0.150	-15.31

The result of Thermodynamic parameters, i.e. Free energy change (ΔG), Enthalpy change (ΔH) and Entropy change (ΔS), were presented in (table 4.2-4.4) and the values of the parameters have been calculated using standard equations mentioned in 4 and 5 respectively and summarized in the table above i.e. 4.2-4.4. The negatives values of (DG) obtained in both cases reveal that the adsorptions of dyes are thermodynamically feasible and spontaneous. The positives values of (ΔH), confirm the endothermic nature of the adsorption process. The positive values of (ΔS), reflect the affinity of MB and MO towards SSL and JL onto AC-SSLA, JLA, SSLB and JLB and indicate that the randomness increased at the solid/solution interface during the adsorption process.

A plot of lnk (on the y-axis) and 1/T (on the x-axis) yielded a straight line, from which A was obtained based on the intercept value for both MB and MO dye (Ayuba *et al.*, 2014). The values of k from the plots, increases with temperature decrease. Since adsorption capacity increases with increasing in temperature, for both MB and MO it can therefore be concluded that the adsorption capacity decreases with increasing temperature for the same mass of adsorbent and analyte concentration. The decrease was due to weak adsorptive forces between the active sites and the adsorbed species and also between close by molecules of adsorbed phase. This suggests that the adsorption process is physisorption (Yunus *et al.*, 2021).

Table 4.5: kinetics studies parameters of methylene blue dyes of jute and sickle senna leaves, raw samples acid and base activation.

	Pseudo first order	Pseudo second order	Ipdm	Elovic
AC-MBSSLA **q_e (exp.) = 34.15**	q_e= 30.60 (mg/g) k_1=0.00303(min1) R^2= 1.00	q_e= 34.32 (mg/g) k_2=0.00061(mg/min) R^2=1.00	K_{id}= 0.867 C= 9.343 R^2= 0.7840	B= 0.113 A= 0.0458 R^2=0.7844
AC-MBSSLB **q_e (exp.) = 32.58**	q_e= 22.99 (mg/g) k_1=0.0320(min-1) R^2= 1.00	q_e= 31.98 (mg/g) k_2=0.00041(mg/min) R^2=1.00	K_{id}= 0.965 C= 11.076 R^2= 0.8840	B= 0.313 A= 0.422 R^2=0.9378
AC-MBJLA **q_e (exp.) =39.63**	q_e= 32.88 (mg/g) k_1=0.0220(min-1) R^2= 1.00	q_e= 31.77 (mg/g) k_2=0.0061(mg/min) R^2=1.00	K_{id}= 1.64 C= 13.722 R^2= 0.8034	B= 0.115 A= 0.025 R^2=0.8035
AC-MBJLB **q_e (exp.) = 32.63**	q_e= 21.54 (mg/g) k_1=0.370(min-1) R^2= 1.00	q_e= 31.77 (mg/g) k_2=0.0067(mg/min) R^2=1.00	K_{id}= 0.867 C= 8.56 R^2= 0.9935	B= 0.316 A= 0.0458 R^2=0.9935
AC-MOSSLA **q_e (exp.) = 34.49**	q_e= 28.43 (mg/g) k_1=0.474(min-1) R^2= 0.7554	q_e= 30.57 (mg/g) k_2=0.0840(mg/min) R^2=0.9907	K_{id}= 0.967 C= 10.54 R^2= 0.8890	B= 0.478 A= 0.068 R^2=0.9277
AC-MOSSLB **q_e (exp.) = 33.04**	q_e= 28.54 (mg/g) k_1=0.660 (min-1) R^2= 0.9880	q_e= 34.00 (mg/g) k_2=0.0065(mg/min) R^2=0.9612	K_{id}= 12.108 C= 16.37 R^2= 0.9939	B= 0.147 A= 0.072 R^2=0.9375
AC-MOJLA **q_e (exp.) = 34.16**	q_e= 20.76 (mg/g) k_1=0.520(min-1) R^2= 0.9621	q_e= 31.89 (mg/g) k_2=0.0034(mg/min) R^2=0.8429	K_{id}= 2.299 C= 7.897 R^2= 0.8579	B= 0.796 A= 0.227 R^2=0.7844
AC-MOJLB **q_e (exp.) = 34.16**	q_e= 29.43 (mg/g) k_1=0.430 (min-1) R^2= 0.9979	q_e= 33.88 (mg/g) k_2=0.0035(mg/min) R^2=0.9552	K_{id}= 11.39 C= 19.17 R^2= 0.9732	B= 0.131 A= 0.016 R^2=0.9354

AC-MOSSLR **q_e (exp.) = 34.54**	q_e= 30.44 (mg/g) k_1=0.0967(min-1) R^2= 0.9910	q_e= 34.34 (mg/g) k_2= 0.193 (mg/min) R^2=0.9802	K_{id}= 0.978 C= 9.099 R^2= 0.9878	B= 0.109 A= 0.0148 R^2=0.9878
AC-MBSSLR **q_e (exp.) = 35.61**	q_e= 30.76 (mg/g) k_1=0.064 (min-1) R^2= 0.9910	q_e= 34.66 (mg/g) k_2= 1.091 (mg/min) R^2=0.9802	K_{id}= 0.876 C= 6.20 R^2= 0.9184	B= 0.161 A= 0.0128 R^2=0.9184
AC-MBJLR **q_e (exp.) = 33.56**	q_e= 29.23 (mg/g) k_1=0.0875(min-1) R^2= 0.9328	q_e= 34.12 (mg/g) k_2= 1.44 (mg/min) R^2=0.9969	K_{id}= 0.8613 C= 5.40 R^2= 0.9668	B= 0.185 A= 0.0148 R^2=0.9668
AC-MOLR **q_e (exp.) = 33.63**	q_e= 28.23 (mg/g) k_1=0.0645(min-1) R^2= 0.9561	q_e= 32.98 (mg/g) k_2=0.3081(mg/min) R^2=0.8229	K_{id}= 0.7228 C= 8.334 R^2= 0.9583	B= 0.123 A= 0.0137 R^2=0.9625

The Pseudo first order, Pseudo second order, Simple elovich and Intra particle diffusion were used to determine the rate constant for adsorption of jute leaves and sickle senna leaves onto Methylene blue and methyl orange dyes. the results were presented in the figure above and the parameters were summarized in the tables above i.e. 4.5 the results shows that the correlation coefficients (R^2) of Pseudo first order and Pseudo second order adsorption model are high than that of simple elovich and intra particle model using methylene blue in all the adsorption process while using methyl orange the correlation coefficient (R^2) is high in elovich model and intra particle diffusion model than that of Pseudo first order and Pseudo second order in all the adsorption process, also all the experimental data of the amount of methylene blue and methyl orange adsorbed on SSL, JL and AC-SSLA, JLA, SSLB and JLB at the equilibrium time are much closer to that of the calculated data.

Table 4.6: Adsorption Isotherms Parameters.

ADSORBENT	LANGUMAIR	FREUNDLICH	TEMKIN	D.R
AC-MBSSLA	q_m=198.17(mg/g) K_L= 0.722 (L/mg) R^2= 0.9996	n= 0.066 K_f= 6.84 R^2= 0.7766	b_T= 74.11(Kj/mol) K_T= 54.02 (L/mg) R^2= 0.7844	**Q_{max}=49.17(mg/g)** **B= 2.06(Kj^2/mol^2)** **R^2= 0.8300**
AC-MBSSLB	q_m= 209.00(mg/g) K_L= 0.122(L/mg) R^2= 0.9372	n= 0.026 K_f= 4.13 R^2= 0.9454	b_T= 51.78(Kj/mol) K_T= 71.99(L/mg) R^2= 0.9374	**Q_{max}=63.10(mg/g)** **B= 7.06(Kj^2/mol^2)** **R^2= 0.9120**
AC-MOSSLA	q_m=217.33(mg/g) K_L= 0.109(L/mg) R^2= 0.9805	n= 0.615 K_f= 7.65 R^2= 0.9479	b_T=20.494(Kj/mol) K_T= 45.85 (L/mg) R^2= 1.00	**Q_{max}=52.71(mg/g)** **B= 2.06(Kj^2/mol^2)** **R^2= 0.9570**
AC-MOBSSLB	q_m=239.83(mg/g) K_L= 0.079(L/mg) R^2= 0.9645	n= 0.369 K_f= 5.28 R^2= 0.8945	b_T= 20.455(K/mol) K_T= 53.26(L/mg) R^2= 1.00	**Q_{max}=35.12(mg/g)** **B= 3.06(Kj^2/mol^2)** **R^2= 0.9170**
AC-MBJLA	q_m=241.83(mg/g) K_L= 0.042(Lmg) R^2= 0.9770	n= 0.054 K_f= 4.99 R^2= 0.8476	b_T= 85.01 (Kj/mol) K_T= 67.52 (L/mg) R^2= 0.8034	**Q_{max}=33.12(mg/g)** **B= 2.06(Kj^2/mol^2)** **R^2= 0.6890**
AC-MBJLB	q_m=245.82(mg/g) K_L= 0.363(L/mg) R^2= 0.9816	n= 0.055 K_f= 8.02 R^2= 9968	b_T= 78.55 (Kj/mol) K_T= 49.77 (l/mg) R^2= 0.9953	**Q_{max}=61.14(mg/g)** **B= 7.07(Kj^2/mol^2)** **R^2= 0.8620**
AC-MOJLA	q_m=248.50(mg/g) K_L= 0.036(L/mg) R^2= 0.9695	n= 0.498 K_f= 3.18 R^2= 0.9477	b_T=20.50(Kj/mol) K_T= 58.92 (L/mg) R^2= 1.00	**Q_{max}=24.13(mg/g)** **B= 4.06(Kj^2/mol^2)** **R^2= 0.8490**
AC-MOJLB	q_m=217.50(mg/g) K_L= 0.064(L/mg) R^2= 0.9377	n= 0.442 K_f= 5.07 R^2= 0.9275	b_T=12.85(Kj/mol) K_T= 45.78 (L/mg) R^2= 0.0074	**Q_{max}=32.19(mg/g)** **B= 4.06(Kj^2/mol^2)** **R^2= 0.9400**
AC-MOSSLR	q_m=164.67(mg/g) K_L=0.0032(L/mg) R^2= 0.9927	n= 0.499 K_f= 8.57 R^2= 0.7760	b_T=15.37(Kj/mol) K_T= 50.61 (L/mg) R^2= 1.00	**Q_{max}=27.16(mg/g)** **B= 6.06(Kj^2/mol^2)** **R^2= 0.9720**
AC-MBSSLR	q_m= 163.50(mg/g) K_L=0.0032(L/mg) R^2= 0.9971	n=0.132 K_f= 4.58 R^2=0.9243	b_T=15.37(Kj/mol) K_T= 50.08 (L/mg) R^2= 1.00	**Q_{max}=33.13(mg/g)** **B= 4.06(Kj^2/mol^2)** **R^2= 0.9550**
AC-MOJLR	q_m=183.50(mg/g) K_L=0.0033(L/mg)	n= 1.65 K_f= 8.75	b_T=54.74(Kj/mol) K_T= 60.80 (L/mg)	**Q_{max}=32.18(mg/g)** **B= 4.06(Kj^2/mol^2)**

	R^2= 0.9965	R^2= 0.8519	R^2= 0.9668	**R^2= 0.9670**
AC-MBJLR	q_m= 181.33(mg/g) K_L=0.0082(L/mg) R^2= 0.9878	n= 0.119 K_f= 9.64 R^2= 0.9473	b_T=30.80(Kj/mol) K_T= 59.90 (L/mg) R^2= 0.9625	**Q_{max}=39.13(mg/g)** **B= 2.06(Kj^2/mol^2)** **R^2= 0.9850**

The results of isotherms studies for the adsorption of methylene blue and methyl orange dyes were presented in the table 4.3 above and summarized in comparison of the results of isotherms i.e. Langmuir, Freundlich, Temkin and Dubenin redushkebich models, the Langmuir and Temkin model has exhibited a better fit for methylene blue having highst correlation coefficient than Freundlich and Dubenin Redushkebich while Freundlich has a better fit on using methyl orange, having highest correlation coefficent than Langmuir, Temkin and Dubenin Redushkebich.

4.2 REUSABILITY GRAPHS FOR METHYLENE BLUE AND METHYL ORANGE OF BOTH, SSLA&B, JLA&B AND SSLR& JLR, SAMPLES.

In actual environmental applications, the stability and recyclability of jute leaves and sickle senna leaves activated carbon for both raw, acid and base activation system for pollutant/dyes degradation seems particularly important. Repeated use of biochar was evaluated by a multi-cycle experiment using the recycled biochar again directly, and the results are shown in Figure above. In comparison the MO SSLA is little beet good for the reusability in terms of percentage removal of dyes than that of MB SSLA dye as it can be seen in the figure above In short, the prepared adsorbent is of good stability and can still efficiently remove after repeated use.

5. DISCUSSION

6. FOURIER TRANSFORM INFRARED (FTIR) SPECTROSCOPY

The various functional groups that might be participated in the adsorption of MB and MO dyes were elucidatesd using FT-IR analysis in figure 4.1. The FT-IR spectrum reveals a strong broad peak at 3200-3500cm^{-1} indicate the presence of surface hydroxyl group (OH) of both raw JLR and SSLR, and the peak seen at 1600 cm^1 are due to aromatic ring, also peak seen at 1000-1100 are due to primary alcohol of both JLR and SSLR sample, peaks observed at 2800-2900cm^{-1}of both acid and base activation of the sample corresponding to asymmetric C–H stretching of the surface methyl group, usually lignin structure. the absorption band at 2200-2400 cm^1 of both acid and base activation leaves are due to cyanide to nitrogen (CN)or carbon to carbon triple bond of cyanide group, peaks seen at 1600-1700cm^{-1}of both acid and base activation of the leaves are due to presence of C=O from carboxylic acid, Ketone and Aldehyde groups (Shin *et al*., 2008), the peaks seen at 1450-1600cm^{-1}of both acid and base activation of the leaves emerged due to the C=C stretching while the sharp broad peaks at 1050cm^{-1} corresponded to the presence of primary alcohol R-OH.(Wuj and zhang., 2020). The FTIR peaks in both, raw JLR and raw SSLR showed a great deal of similarity and this could be due to same lignocelluloses composition: lignin, hemi cellulose and cellulose ratio. (Ahmad and Rahman., 2011).

Conversely, after pyrolysis at 350°C of the both leaves, most of their surface functionalities were hardly retained. However, the acid and base activation leaves showed a broad absorbance peak within 1500-1000cm^{-1}due to C-H bending (Auta *et al*., 2014). This is vividly shown in Fig. 2.The FTIR spectra of oxygen functionalized leaves.

7. SCANNING ELECTRON MICROSCOPY (SEM)

The SEM microscopic images of the precursor SSL, JL and AC-SSLA, SSLB, JLA and JLB were shown in the (figure 4.12 to 4.26) the SSLR and JLR adsorbent shows irregular surface and low degree of porosity (figure 4.4 and 4.5) while, AC-SSLA, JLA, SSLB and JLB represents the highly porous structure with small number of microspores. It's probably as a result of evaporation of volatile organic compounds during pyrolysis and activation process. (Figure 4.6 to 4.9). Therefor such type of porous structure was responsible for the enhance removal of MB and MO dyes from aqueous phase. AC-SSLA, SSLB, JLA and JLB are filled due to the adsorption of MB and MO dyes which may confirm the adsorption phenomenon between MB and MO dyes on SSL and JL.

8. EFFECT OF CONTACT TIME

The effect of contact time on the adsorption of methylene blue and methyl orange dyes removal from aqueous solution were presented in the figure 4.36 to 4.40. it was seen clearly that the maximum adsorption occurred in 10-20 minute and after 30 minutes, an equilibrium state was obtained for the adsorption of methylene blue and methyl orange, while it occurred in 10-30 minute: an equilibrium state was obtained for adsorption of both MB and MO. Initially due to high concentration gradient and more available adsorption sites, the rate of dye removal was high. The rate of dye removal shows an increased in percentage removal with increase in contact time and this process continues until the adsorption process reaches equilibrium i.e. 30 minutes for MO and MB. After reaching the equilibrium, i.e. as the time proceeds no further uptake of adsorbate by adsorbent will occur (Ayuba and Idoko., 2021), the first step took 10–30 min to reach the relative adsorption equilibrium state called fast adsorption. The performance was due to the binding force between MB& MO dye and the adsorption active sites, and functional groups as well on the SSLA&B and JLA &B adsorbent were fully and efficiently completed. The absorption rate of the dye was controlled by the rate of the dye transported from the solution to the surface of the adsorbent particles (Amin., 2008). The second step was called slow adsorption process. After 30 min of contact time, the relative increase in the removal extent of MB & MO was not significant, and with the increase in contact time, the adsorption rate increased and gradually stabilized. This performance was due to the binding force between MB & MO dye and the adsorption active sites, functional groups as well on the SSLA&B and JLA&B adsorbent were gradually saturated (Chartarraya, *et al*., 2013). The absorption rate of the dye was controlled by the rate of the dye transported from the exterior to the interior pore sites of the adsorbent particles, more over the lower the dye initial concentration the shorter the time to achieved the adsorption equilibrium state. The results were basically consistent with previous studies on the removal rate of dyes (Cuevas. *et al*, 2010).

8.1.1. EFFECT OF TEMPERATURE

In order to optimized the system temperature for the maximum removal efficiency, experiment have been conducted at different temperatures 299 K, 303K, 308k, 313K, and 318K by keeping other parameters constant such as pH 2 equilibration time 3 minute for MB and MO 35 minute, adsorbent dose of 0.7g for MB and 0.6g for MO. experimental results regarding the effect of temperature were carried out in (figure 4.40 to 4.44), from the results obtained it shows that the percentage removal increase as the temperature of the solution also increased which indicates that the adsorption process is endothermic in nature. Better adsorption at higher temperature may be due to the acceleration of some originally slow adsorption steps or due to retardation of the process such as aggregation of molecules, association of ions and complex formation in the system because of thermal agitation, these indicate that the adsorption is favored at high a temperature which is true for an endothermic process. An increase in temperature normally enhances the diffusion rate of adsorbate molecules within the pores of the adsorbent due to the increased kinetic energy of

the solute. Similar effect in temperature was previously reported on adsorption of MG onto eggshells (Bulut and Aydin., 2006) on polyvinyl alcohol activated carbon.

9. EFFECT OF PH

In addition, the dissociation degree of H+ by the oxygen-containing functional groups on the surface of the SSLA&B JLA &B adsorbent increased with the increase of pH, which increased the electro negativity of SSLA&B JLA &B adsorbent and the electrostatic attractive force between the dye cation and SSLA&B and JLA&B. The fact that the free hydrogen ions inhibited the adsorption reaction of dye cat ion onto AC site by competing adsorption, could lead to a reduction in MB and MO removal rate. The increase in the concentration of hydroxide ions in the solution made the dissociation degree of MB small, thus the removal rate of MO was improved as the pH value increased (Zheng and sun., 2014). In addition, the dissociation degree of H+ by the oxygen-containing functional groups on the surface of the JLA&B adsorbent increased with the increase of pH, which increased the electro negativity of JLA&B adsorbent and the electrostatic attractive force between the dye cat ion and JLA&B adsorbent.

The influence of pH solution on the adsorption of dye by jute leaves and sickle senna leaves is favored by increasing the initial pH solution; the dye removal efficiency was increased. As the solution pH was raised, the surface functional groups on the adsorbents were de protonated and it changes to negatively charged surface (Ojedokun and Bello., 2009), the MB and MO dye molecules in the aqueous solution have the positively charged ions. The increase of MO removal at higher pH may be due to the electrostatic attraction forces between the positive charged dye molecules and the negatively charged surface adsorbent, while the decreased in the dye removal at pH 10 of MB dye is due to the lesser electrostatic attraction between the positive and negative charge on the surface of the adsorbent (Dhorabe *et al*., 2015). The solution pH of 10 was the optimum condition to eliminate MB and MO dye with both Jute and sickle senna leaves acid and base Modified (Shin *et al*., 2008) reported that MO removal by various sorbents was increased with increasing pH solution.

10. EFFECT OF INITIAL DYE CONCENTRATION

The adsorption of methylene blue onto the activated carbon was studied for different concentrations 10, 20, 30, 40 and 50 of MB and MO solution. The data obtained are provided in the table 15, The experiment was conducted at optimum condition 0.6gm adsorbent dosage, 35 ℃ and 4 pH for contact time of 50 min. Maximum dye removal occurred in the initial concentration of methylene blue and methyl orange showed gradual reduction when initial concentration of Methylene blue and methyl orange was raised. It could be ascribed to fixed concentration of adsorbent dosage with increase in initial dye concentration the adsorption sites were fixed and achieved saturation at low dye concentration. Hence with increase in dye concentration no further adsorption could be achieved and resulted in reduced removal of dye with increase in dye concentration. The removal extent of dyes was decreased with an increase in the initial MB and MO concentration due to the lack of available active sites under high concentration of MB and MO (Mondal and kar., 2008), whereas the adsorption capacity of MB and MO on both JLA&B and SSLA &B increased with the increase of initial MB and MO concentration. An increase in initial dye concentration may be resulted in the decreasing dye uptake due to reduction in ratio of sorbent active surface to the adsorbate molecules, (Bello and Ahmad., 2012).

11. EFFECT OF ADSORBENT DOSAGE

The amount of adsorbent dosage was varied in the given range 0.2gm, 0.4gm, 0.6gm, 0.8gm & 1 gm. It was observed from the graphs that increasing the dosage increased the % removal of methylene blue and methyl orange, as there was no drastic increase in the adsorption rate on increasing the dosage of adsorbent beyond 0.6gm of activated carbon, hence, from economic point of view, 0.6gm was taken as optimum dosage for removal of methylene blue and methyl orange. It can be attributed to the increase in adsorbent sites for more adsorption of the dye at the fixed 20mg/L, the removal rate of MB and MO gradually increased due to the increases of the number of adsorbent pores and adsorption sites (Sadiq *et al*., 2016). Ayuba *et al*. (2021), reported that, the adsorption would tend to equilibrium when the mass of adsorbent reached a certain value. The removal rate of MB and MO reached the saturated value at adsorbent mass of 30mg corresponding to the initial MB and MO concentration of 30mg·L−1, respectively. At high adsorbent dosages, the available number of MB and MO dye molecules in solution was not enough to completely combine with all effective adsorption sites on the adsorbent, resulting in a surface equilibrium state and a reduction in the adsorption capacity per unit mass of adsorbent (Dhorabe *et al*,. 2015).

12. THERMODYNAMICS PARAMETERS

Thermodynamics parameters, i.e. free energy change (ΔG), enthalpy change (ΔH), entropy change (ΔS), vary with thermodynamics equilibrium constant (Kc) the curve was presented in (table 4.42) and the values of parameters has been calculated using standard equation mentioned in equation 7 to 9, Respectively. The negative values of (ΔG) obtained in both cases reveal that the adsorptions of dyes are thermodynamically feasible and spontaneous, positive values of (ΔH) confirm the endothermic nature of the adsorption process. on increasing temperature, the degree of the adsorption increase. The numerical values of ΔH also predict the chemisorptions behavior of this adsorption process. The positive values of DS reflect the affinity of MB and MO towards SSL, JL and AC-SSLA, SSLB, JLA and JLB and also indicate randomness is increased at solid/solution interface during the adsorption process (Ladan *et al*., 2013), (Ayuba *et al*, (2021): MB,Ibrahim, (2019).

13. KINETICS STUDIES

The kinetics studies of any adsorption system describe the rate of adsorbate uptake on adsorbent, and it controls the equilibrium time. The kinetics parameters are helpful to give information about uptake rate, which gives information for designing and modeling the adsorption process.

The mechanisms and rate determining step of an adsorption reaction can be determined by modeling in to kinetics models. The Pseudo- first order, Pseudo-second order, Intra-particle diffusion and Simple Elovich models were used to determine the rate constant for the adsorption of jute leaves and sickle senna leaves onto methylene blue and methyl orange, the best fit kinetics model is mainly selected on the linear regression correlation coefficient (R^2), of pseudo first order adsorption model and pseudo second order kinetics model is higher than that of intra-particle diffusion and simple elovich in all cases. The experimental data of the amount of methylene blue and methyl orange adsorbed on SSL, JL onto AC-SSLA, SSLB, JLA and JLB at equilibrium time are much closer to that of calculated data. It's concluded that the adsorption of methylene blue and methyl orange is best described by the pseudo-first order and pseudo second order equation, It's also concluded that the rate limiting step may be the chemical reaction but not the mass transport (Audu *et al*., 2014).

14. ISOTHERMS

Adsorption isotherms provide helpful information to identify the uptake mechanisms and characteristics of the adsorbent surface for design of sorption system. The adsorption isotherms used to describe the experimental data are; Freundlich, Langmuir, Dubinin Radushkevich and Temkin isotherm models. The goodness of fit of the experimental data was measured by the correlation coefficient, R^2 for all the temperatures ; 299, 303, 308, 313 and 318 respectively, in comparisons with dyes methyl orange (MO) showed a higher removal for both acid and base activation compare to that of methylene blue (MB), which Indicate its goodness for the adsorption of dyes on activated carbon over a methylene blue dye, while on comparisons with isotherms, Freundlich and Langmuir showed better fit than Temkin and dubinin Radushkevich adsorption isotherm model in which the R^2 in freudlich and Langmuir is relatively high in both sickle senna and jute leaves acid and base activation of MB and MO dyes which can describe the experimental data accurately. In addition, AC of jute leaves and sickle senna leaves has a homogeneous surface, and the adsorption of Methylene Blue and methyl orange is in monolayer coverage because of its homogeneous nature.

The adsorption bond between adsorbent and adsorbate would be relatively strong if the value of n, acquired from the Freundlich isotherm, is more than one (Kansal and kumara., 2014). Therefore, the n values of 1.65 and above obtained by this isotherm model showed that MB and MO were properly adsorbed by jute and sickle senna leaves for both acid and base activation. Freundlich isotherm model assumes a non-ideal adsorption on heterogeneous surface of bio sorbent (Ayuba *et al*., 2021), in the present study, the experimental data best obey Freundlich isotherm and adsorption is physisorption, the adsorption is a typical multilayer and hence the surface of the used adsorbent is heterogeneous. Similar R^2 values were obtainable in the related literature (Auta and Hameed., 2014).

15. CONCLUSION

This study shows that the jute and sickle senna leaves activated carbon is essential for the removal of dyes, with the high Adsorption capacity of AC-MOJLA 248 followed by AC-MBJLB 245 respectively.

The experimental data for all studied dyes were found to closely fit pseudo first order and second order kinetics model, followed by simple elovic model, the methyl orange methylene blue dye adsorbed onto jute and sickle senna leaves activated carbon closely fitted the Langmuir and Temkin isotherm model, the adsorption of MO and MB dyes on to the activated carbon of jute and sickle senna leaves was spontaneous and feasible because ΔG is negative, the positive values of ΔS indicated that the randomness of the solid/solution interface increased during the adsorption process, the adsorption process of all the dyes was endothermic because ΔH is positive.

The FTIR and SEM analyses of the adsorbent suggest that adsorption of the dyes was through an electrostatic interaction between the functional groups present in the dyes and those on the surface of the adsorbent. The results of the presents study substantiate that the bio- waste based materials of JL and SSL is promising adsorbents for the removal of methylene blue and methyl orange dyes.

In actual environmental applications, the stability and recyclability of jute and sickle senna leaves activated carbon for both raw, acid and base activation system for dyes degradation seems particularly important. Repeated use of biochar was evaluated by a multi-cycle experiment using the recycled biochar again directly, these studies indicate that jute leaves and sickle senna leaves is comparable to other plant for it good removal of dyes/effluence in the treatment of waste water, effort should be made to commercialized its production,

this work shows that activated carbon of jute and sickle senna leaves could be used as substitute for conventional activated carbon in the treatment of waste water, air purifications, environmental project, food decolorisations, gold extraction and solvent extractions.

Funding:

The research received no external funding.

Conflict of interest:

The authors declare no complicit of interest.

Data Availability Statement:

The data is available online via the respective reference

AI Usage Disclosure:

No AI tools were used in the preparation of this manuscript.

Authors Contribution;

Salisu Hassan Nahuche; writing original draft

Magaji Ladan; writing review and editing

REFERENCES

[1] Abdullahi M.A. and Bridget I. (2021). (kinetics, equilibrium and thermodynamics studies of congo red dye adsorption from aqueous solution onto activated cowpea (*vigna unguiculata*) husk.algerian *journal of chemical engineering*. **130; 12-14**

[2] Acharya J. Sahu JN. Sahoo BK, Mohant CR. Meikap BC. (2009). Removal of chromium (vi) from wastewater by activated carbon developed from tamarine wood activated with zinc chloride,*JornalofChemicalEngineering*. **150:25–39**

[3] Adelaji O, A. Bankole, A.C Oladipo, M.E lane, OB (2019). Biosorption of Hg (ii) Ions. Congo red and their Binary mixture, using raw and chemically activated mango leaves. *International journal of energy and water resources*, **3(1), 1-1**

[4] Ahmad, M.A, Rahman N.K, (2011). Equilibrium, kinetics and thermodynamic study of Remazol Brilliant orange 3r dye adsorption of coffee husk-based activated carbon. *Jornal of Chemicalengineering***170:154–161**

[5] Amin, N.K. (2008). Removal of Reactive Dye from aqueous solutions by adsorption, onto activated carbons prepared from sugarcane bagasse pith. Desalination. **223, 152–161**

[6] Asheik Mideen, (2015). Adsorption of Methylene Blue Dye on Activated Carbon from rice husk., *journal of chemical and pharmaceutical research*. **7(2):761-765**

[7] Auta, M.B.H. Hameed, Chitosan–Dlay (2014). Compo3site, as highly effective and low - cost Adsorbent, for batch and fixed-bed adsorption of methylene Blue. *Jornal of Chemical engineering*. **2014, 237, 350–361**

[8] Ugbe, F.A. Adamu S. O and Aloysius A.P. (2014). Thermodynamic study of the competitive adsorption of chromium (iii) ions and halides onto sweet orange (citrus sinensis) peels as adsorbent. *International jornal of Environmental and Analytical chemistry*. **2(4), 1-4**

[9] Bello, O.S. Semire B. (2012). Equilibrium, kinetic and quantum chemical studies on the adsorption of congo red using *Imperata cylindrica* leaf powder activated carbon. *Jornal of toxicology and Enviromental chemistry*. **94:1114–112**

[10] Bello, O.S. (2013). Adsorptive Removal of Malachite green with activated carbon prepared from oil palm fruit fibre by koh activation and co_2 gasification. *Jornal of Industrial chemistry*. **66:32– 41**

[11] Bello, O.S. Ahmad M.A, siang, T.T. (2011). Utilization of cocoa pod husk for the removal of Remazol black b reactive dye from aqueous solutions: kinetic,equilibrium and thermodynamic studies. trends appl sci res **6(8): 794–812**

[12] Bello, O.S Adeogun I.A Jaelu J.C. (2008). Adsorption of methylene blue onto activated carbon derivedfrom periwinkle shells: kinetics and equilibrium studies. chem ecol **24:285–295**

[13] Bello, O.S Ahmad M.A (2011a). Response surface modelling and optimization of Remazol brilliant blue reactive dye removal, using periwinkle shell-based activated carbon. sep sci technology **46(5):2367–2379**

[14] Bello, O.S Ahmad, M.A (2011b). Adsorption of dyes from aqueous solution using chemical activatedmangopeels. Second international conference on environmental science and technology (icest), **vol 2, pp 108–113**

[15] Bello, O.S Ahmad M.A. (2012a). Preparation and characterization of activated carbon derived from rubber seed coat. bulg j sci edu **21:389–395**

[16] Bello, O.S Ahmad M.A. (2012b). Coconut (cocos nucifera) shell based activated carbon for the removal of malacite green dye from aqueous solutions. sep sci technol 47:903–912

[17] Bulut, y. Aydin, H.A (2006). Kinetics and thermodynamics study of methylene blue adsorption on wheat shells desalination. **194, 259–267**

[18] Baiocchi, M.C. Brussino, E. Pramauro, A.B. Prevot, L. Palmisano, G. Marcì, (2020). Characterization of methyl orange and its photocatalytic degradation products by HPLC/UV–VIS

[19] Bulut, Y. Karaer, H. (2020). Adsorption of Methylene Blue from Aqueous Solution by Crosslinked Chitosan/Bentonite Composit, *Chemical Engineering Journal*. **114(9):4993– 5010**

[20] Chartarrayawadee, W. Moulton, S. Too, C. Wallace, G. (2013). Fabrication of Graphene Electrodes by Electrophoretic Deposition and Their Synergistic Effects with PEDOT and Platinum, Chiang Mai J. Sci., **40, 750-762, 2013**.

[21] Chemical Composition of Sickle Pod (Senna obtusifolia) and Coffee Senna (Senna occidentalis) Leaves Indigenous to Mubi *New York Science Journal 2018;* ***11(7),*** http://www.sciencepub.net/newyork

[22] Cuevas, L.Villacura, E. Toloza, C. Magellan Peat. (2010). *Sphagnum Magallanicum*, as Natural Adsorbentof Recalcitran Synthetic Dyes, J. Soil Sc. Plant Nutr**., 8,31-43, 2008.**

[23] Dhorabe, P. Lataye, D. Ingole, R. (2016). Removal of 4-nitrophenol from aqueous solution by adsorption onto activated carbon prepared from Acacia glauca sawdust, Water Science & Technology. doi: **10.2166/wst.2015.575**

[24] *Directorate General of Commercial Intelligence and Statistics (DGCI&S), 2020. India (Kolkata)*

[25] Dorothy A. sheik mideen,(2015). Adsorption of methylene blue dye on activated carbon from rice husk,,journal of chemical and pharmaceutical research, **7(2):761-765**

[26] ema.europa.eu/medicines/herbal/sennaefolium

[27] *European Medicines Agency, Journal of Herbal and Medicinal Plant Leaves.(2020)*

[28] Fu, J. Chen, Z. wang, M. S. zhang, J. Zhang, j. han, R. (2016). Aadsorption of Methylene blue by a high-efficiency adsorbent (polydopamine microspheres): kinetics, isotherm, thermodynamics and mechanism analysis. Jornal of Chemical Engineering. **259, 53–61**

[29] Gimba c, musa I. (2007). Preparation of activated carbon from agricultural waste: cyanide bindingwithactivated carbon matrix from coconut shell. j chem nigeria 32:167–170

[30] Haddad, M. Mamouni, R. Saffaj, N. Lazar, S. (2002). Removal of a cationic dye – Basic Red 12– from aqueous solution by adsorption onto animal bone meal, Journal of the Association of Arab Universities for Basic and Applied Sciences, 12, 48–54, 2012.*International Journal of Mass Spectrometry*, **(214) 247-256.**

[31] *International Legume Data Base & Information Service (ildis) (2005): Senna tora (l.) roxb. version 10.01, november 2005. retrieved 2007-dec-20.*

[32] Kansal S.K, kumari A. (2014). Potential of m. oleifera for the treatment of water and wastewater.

[33] Karaer Yağmur (2020). Preparation and Characterization of Polyvinyl Alcohol/Activated Carbon (PVA/AC) Composite and Its Use in the Adsorption of 4-Nitrophenol (4-NP), ADYU J **SCI, 10(1), 160-178**

[34] Ladan, M. Ayuba, A.M. Bishir, U. Jamilu, A. and Habibu, S. (2013). Thermodynamic properties of chromium adsorption by sediments of river watari, kano state (chemsearch *journal* **4(1): 1 – 5,** *publication of chemical society of nigeria, kano chapter*

[35] M.M El-halwany, (2010). Study of Adsorption Isotherms and kinetic models for Methylene blue on activated carbon developed from egyptian rice husk (part ii), *international journal of science and technology of desalting and water purification*.

[36] Mondal, N.K. Kar, S (2018). Potentiality of banana peels for removal of congo red dye from aqueous solution: isotherm, kinetics and equilibrium studies. *Journal of Applied water science*, **8(6) 1-12.**

[37] Muhammad Bashir Ibrahim. B.sc. M.sc., PhD (buk) professor of physical chemistry. Water pollution and the quest or its remediation: the natural resource option, professorial inaugural lecture. (2019)

[38] N. Muhamad, J M.D Smith, D. (2018). Nanotubes synthesis by Fenton's reagent method and their potential application for removal of azo wedc conference sanitation and water for all, Islamabad, pakistan, , **pp. 346–349**

[39] Naggar, N. Hussein, M., El-Sawah, A. (2018). Phycobiliprotein-mediated synthesis of biogenic silver nanoparticles, characterization, in vitro and in vivo assessment of anticancer activities, Scientific Reports, **doi:10.1038/s41598-018-27276-61.**

[40] *Nature serve (2007): senna tora (l.) roxb. species factsheet. version 6.3, 2007-oct-29. retrieved 2007-dec-20.*

[41] Nourmoradi H. Khiadani M. Nikaeen M. (2013**)**. Multi-component Adsorption of Benzene, Toluene, Ethyl Benzene and Xylene from aqueous solutions by montmorillonite modified with tetra Decyl tri methyl Ammonium Bromide. *Journal of chemistry***, (203), 1-1**

[42] Ojedokun, A. T., Bello, o. s. (2019). Functionalization of Powdered Walnut Shell.

[43] Ojo, T. A. Ojedokun, A. T.,Bello, O. S. (2019). Functionalization of powdered walnut shell.

[44] Ojo, Wen-da oh, A.V., Xiao Chen, Rohana Adnan, Jun-Wei lim, Kah-Hon Leong, Teik-Thye lim (2019). Catalytically active nitrogen-doped porous carbon derived from biowastes for organics removal via peroxymonosulfate activation. *chemical engineering journal.* **374, 11.**

[45] Olugbenga Solomon Bello, Kayode Adesina Adegoke and Opeyemi Omowumi Akinyunni (2017). Preparation and Characterization of a Novel Adsorbent from Moringa Oleifera leaf, appl water sci (**7)1295–1305**.

[46] Paralikar, P.(2014). Biogenic Synthesis of Silver Nanoparticles Using Leaves Extract of EpiphyllumOxypetalum and its Antibacterial Activity, Austin. *Journal of Biotechnology and Bioengineering***, (1) 22-24**

[47] Puthoor S. (2017). Adsorption of Methyl Orange on Activated, Carbon Influence of Cerium Oxide Loading (Unpublished master's thesis). University of Calgary, Calgary, AB. doi:**10.11575/PRISM/24716 http**

[48] Rodr Iguez, J. Garc´I.A, Govejero, and M. Mestanza (2009). Adsorption of Anionic and Cationic dyes on Activated carbon from aqueous solutions: equilibrium and kinetics," journal of hazardous materials, **vol.172, no.2-3, pp.1311–1320, 2009.**

[49] S. Chen, J. Zhang, C. Zhang, Q. Yue, Y. Li, C. Li, (2010). Equilibrium and kinetic studies of methyl Orange Equilibrium Studies and Kinetics Mechanism for the Removal of Basic and reactive dyes in both single and binary systems using EDTA Modified Rice Husk," International Journal of Physical Sciences. **vol.5,no.5,pp.582–595,2010**

[50] Sadiq D. Attahir, I. Mustapha B.I. and Ayuba A.M. (2016). Thermodynamic Studies of lead (ii) ion Adsorption by the Shell of Sweet Dattock (Detarium microcarpum) 6International Journal of Chemical and Natural science9 vol. 4, **no. 1 (2016): 374-378**

[51] Saikia A. Banerjee S. and Veer V. (2015). Adsorption Isotherm, thermodynamic and kinetic study of arsenic (iii) on iron oxide coated granular activated charcoal, International Research Journal of Environmental Sciences, **2319–1414 vol. 4(1), 64-77**,

[52] Senthil Kumaar (2005). Adsorption of Methylene Blue onto Jute Fiber Carbon: Kinetics and Equilibrium Studies.", Journal of Colloid and Interface Science. volume**: 284, issue: 1, pages: 78-82**

[53] Shin, M.C Kim, H. D Jeon, C. S; Baek, K (2008). Removal Characteristics of Reactive Black Using Surfactant-Modified Activated Carbon. *Journal of Water Desalination*, **(4) 20- 223**,

[54] Umar Y. Bishir U. Muhammad B. I. (2020). Kinetic and thermodynamic studies of malachite green adsorption using activated carbon prepared from desert date seed shell. *Algerian Journal of engineering and technology*, **(6) 2-6**

[55] Umar Y. Bishir U. Muhammad B.6I. (2021). Experimental and quantum chemical investigation for the single and competitive Adsorption of cationic dyes on to the activated carbon. *Algerian Journal of Engineering and Technology*, **(21) 6-8**

[56] Wandal. (2018). Insights Into the Thermolytic Transformation of Lignocellulosic Biomass Waste to Redox-active Carbocatalyst: durability of surface-active sites. *appl catal*, *b*. **233, 120-129.**

[57] WuJ., Zhang, Z., Xu J, Wang, C. Yuan, h., (2020). Adsorption of Congo red by bg. Bioresources. **(3) 6928-6940.**

[58] zheng, H.,Sun, Q. Y (2020). Biosorbent Prepared from Pomelo Peel by Hydrothermal Technique and its Adsorption Properties for congo red. *Materials research express*, **7(4), 045505**.